Published in final edited form as:

J Immunol. 2023 December 15; 211(12): 1792–1805. doi:10.4049/jimmunol.2300303.

HLA-DQ8 Supports Development of Insulitis Mediated By Insulin-Reactive Human TCR-Transgenic T-cells In NOD Mice[1]

Jeremy J. Racine[*], **Adel Misherghi**[*,†], **Jennifer R. Dwyer**[*], **Richard Maser**[*], **Elvira Forte**[*], **Olivia Bedard**[*], **Susanne Sattler**[‡,§], **Alberto Pugliese**[¶], **Laurie Landry**[‖], **Colleen Elso**[#], **Maki Nakayama**[‖], **Stuart Mannering**[#], **Nadia Rosenthal**[*,‡], **David V. Serreze**[*]

[*]The Jackson Laboratory, Bar Harbor, Maine, USA

[†]College of the Atlantic, Bar Harbor, Maine, USA

[‡]Imperial College London, London SW7 2AZ, UK

[§]Medical University Graz, 8036 Graz, Austria

[¶]Diabetes Research Institute, Miller School of Medicine, University of Miami, Miami, FL

[‖]Barbara Davis Center for Childhood Diabetes, University of Colorado School of Medicine, Aurora, CO, USA

[#]Immunology and Diabetes Unit, St. Vincent's Institute of Medical Research, Fitzroy, Vic, Australia

Abstract

In an effort to improve HLA-"humanized" mouse models for type 1 diabetes (T1D) therapy development, we previously generated directly in the NOD strain CRISPR/Cas9-mediated deletions of various combinations of murine MHC genes. These new models improved upon previously available platforms by retaining β2m functionality in FcRn and nonclassical MHC I formation. As proof of concept, we generated H2-D^b/H2-K^d double knockout NOD mice expressing human HLA-A*0201 or HLA-B*3906 class I variants that both supported autoreactive diabetogenic $CD8^+$ T-cell responses. In this follow up work, we now describe the creation of ten new NOD based mouse models expressing various combinations of HLA genes with and without chimeric transgenic human TCRs reactive to proinsulin/insulin. The new TCR-transgenic models develop differing levels of insulitis mediated by HLA-DQ8 restricted insulin reactive T-cells. Additionally, these transgenic T-cells can transfer insulitis to newly developed NSG mice lacking classical murine MHC molecules, but expressing HLA-DQ8. These new models can be utilized to test potential therapeutics for a possible capacity to reduce islet infiltration or change the phenotype of T-cells expressing T1D patient derived ß-cell autoantigen specific TCRs.

Introduction

Despite a successful history in mapping the cellular and genetic underpinnings of type 1 diabetes (T1D)[4], the NOD mouse has been less successful as a pre-clinical model in the

[1] Correspondence: Dr. David Serreze, PhD, The Jackson Laboratory, 600 Main St., Bar Harbor, Maine 04609, dave.serreze@jax.org, (207) 288-6403.

development of disease therapeutics (1). In an effort to improve the NOD mouse as a pre-clinical platform, we have undertaken previous efforts at HLA-"humanizing" the strain (2–5). This work indicated that after HLA-"humanization", T1D patient-relevant autoreactive T-cells can develop and function within the NOD environment (5, 6). However, the early generations of HLA-"humanized" NOD mouse models relied upon *β2m*$^{-/-}$ mutations to eliminate murine MHC I expression. This approach, while effective, introduced unintended effects on immune cell functionality and therapeutic development (7). β2m is also critical for both non-classical MHC formation and the various roles of FcRn functionality (8–12), including preventing antibody catabolism (13, 14) and mediating antigen cross-presentation (10). This rendered earlier generation HLA-"humanized" NOD mice poor platforms for development of antibody-based therapeutics. To avoid functional artifacts elicited by *β2m*$^{-/-}$ mutations, we more recently generated direct-in-NOD clustered regularly interspaced short palindromic repeats (CRISPR)/Cas9 mediated murine MHC knockout stocks (7). As part of this work, we generated a series of base models that could be used for introduction of various T1D patient-relevant HLA variants. These included NOD stocks deficient in classical murine MHC class I expression (NOD-*cMHCI*$^{-/-}$) and another additionally lacking murine class II molecules (NOD-*cMHCI/II*$^{-/-}$) (7). As proof of principle, we showed that NOD-*cMHCI*$^{-/-}$ mice can be used as a platform to introduce transgenes encoding T1D patient HLA-A*0201 (HLA-A2) or HLA-B*3906 (HLA-B39) class I molecules and that both supported disease causative autoreactive CD8^{+} T-cell responses (7).

We now report the creation of additional NOD-*cMHCI/II*$^{-/-}$ based models expressing various combinations of HLA class I and II alleles plus or minus transgenes encoding disease relevant human T-cell receptors (hTCR) isolated from T1D patients. Introduction of these hTCR transgenes supports the development of insulitis in NOD-*cMHCI/II*$^{-/-}$ platform mice, in which such lesions are normally absent to minimal. Thus, NOD-*cMHCI/II*$^{-/-}$ -based mice provide new model platforms for introductions of any desired combination of patient-derived HLA and TCR molecules. Additionally, they provide new pre-clinical models to test potential therapeutics that might prevent islet infiltration by patient relevant T-cell populations.

Materials and Methods

Mice

NOD/ShiLtDvs (hereafter, NOD (15)), NOD.Cg-*Prkdc*^{scid} *Il2rg*^{tm1Wjl}/SzJ (hereafter NSG (16)), NOD/ShiLtDvs-*H2-K1*$^{d\text{-}em1Dvs}$ *H2-Ab1*$^{g7\text{-}em1Dvs}$ *H2-D1*$^{b\text{-}em5Dvs}$/Dvs, (hereafter NOD-*cMHCI/II*$^{-/-}$ (7)), NOD/ShiLtDvs-*H2-K1*$^{d\text{-}em1Dvs}$ *H2-D1*$^{b\text{-}em5Dvs}$ Tg(HLA-A/H2-D/B2M)1Dvs/Dvs, (hereafter NOD-*cMHCI*$^{-/-}$-A2 (7)), and NOD.Cg-*Prkdc*^{scid} *H2-Ab1*$^{b\text{-}tm1Doi}$ *Il2rg*^{tm1Wjl} Tg(HLA-DQA1,HLA-DQB1)1Dv/SzJ (hereafter NSG.*H2Ab*^{0}.DQ8 (17)) have all been described previously. NOD.Cg-*Prkdc*^{scid} *H2-Ab1*$^{b\text{-}tm1Doi}$ *Il2rg*^{tm1Wjl} Tg(HLA-DQA1,HLA-DQB1)1Dv Tg(INS*)172Dvs/DvsJ (hereafter NSG.*H2Ab*^{0}.DQ8.hINS), mice

[4]Abbreviations: Clustered regularly interspaced short palindromic repeats, CRISPR; CD4^{-}CD8^{-}, DN; *H2-Ab1*$^{b\text{-}tm1Doi}$, *H2Ab*^{0}; hINS, human proinsulin with a 26-63 ACAGGGGTGTGGGG class I variable number of tandem repeats; HLA-A*0201, HLA-A2; HLA-B*3906, HLA-B39; HLA-DQ8, *DQA*0301 DQB*0302*; Median fluorescence intensity, MFI; T-cell receptors isolated form T1D patient populations, hTCR; Type 1 diabetes (T1D).

are a publicly available unpublished model originally made by The Type 1 Diabetes Mouse Resource (NIH 1UC4DK097610-01) at The Jackson Laboratory (JAX) and were obtained from JAX Mice & Clinical Research Services (strain # 026936). Tg(INS*)172Dvs is a human proinsulin allele with the class I 26–63 ACAGGGGTGTGGGG variable number of tandem repeats sequence associated with T1D development (18). Human insulin and C-peptide were detectable in pancreas of founder Line 172 (Supplemental Table). All mice used in this study were maintained at JAX in a specific-pathogen-free mouse room. Health reports are publicly available at JAX's website. Mice are now additionally screened for segmented filamentous bacterium (19). All procedures involving mice have been approved by JAX's Animal Care and Use Committee. Most incidence studies (unless otherwise noted) were performed using female mice. Flow cytometry experiments utilized a mixture of male and female mice.

Flow Cytometry

Single cell suspensions of splenocytes were prepared by mechanical disruption through 70μm nytex nylon mesh in calcium and magnesium-free HBSS (Sigma-Aldrich; St. Louis, MO) supplemented with 0.5% Hyclone-FBS (ThermoFisher; Waltham, MA) and 2mM EDTA (ThermoFisher). Splenocytes were further treated with Gey's buffer to lyse red blood cells (20). Fc-Shield, anti-CD16/32 (2.4G2, Tonbo, San Diego, CA) was used to block non-specific Fc-receptor binding. For staining, 1×10^6 cells were resuspended in a 1:1 mixture (50uL total volume) of calcium and magnesium-free PBS (supplemented with 0.1% sodium azide and 2% FBS) and Brilliant Stain Buffer (BD Biosciences). After staining, samples were resuspended in calcium and magnesium-free PBS (supplemented with 0.1% sodium azide and 2% FBS) and run on an Attune NxT (ThermoFisher) or FACS-Symphony A5 (BD Biosciences) cytometer. Singlet discrimination was performed by first showing FSC-A vs. FSC-H and gating on diagonal cells, followed by further refinement showing SSC-A vs. SSC-H and gating on diagonal cells. Live/dead discrimination was then performed using propidium iodide vs. FSC-A gating out events positive for propidium iodide. Analysis was performed using FlowJo 10 (BD). Additional gating strategies are described in the respective figure legends.

For intracellular cytokine staining, up to 5×10^6 cells were cultured in RPMI 1640 (ThermoFisher Scientific) media. Cultures were supplemented with 10% heat inactivated Hyclone LOW IgG FBS, 100 μM 2-mercaptoethanol, 1X GlutaMAX, 1mM sodium pyruvate, and 1X MEM NEAA (all from ThermoFisher Scientific), plus 100 U/mL penicillin and 100 μg/mL streptomycin (both from MilliporeSigma). Cells were stimulated for 5 hours at 37°C with 25ng/mL PMA (MilliporeSigma) and 1 μg/mL ionomycin (Cayman Chemical; Ann Arbor, MI), in the presence of a 1/1000 dilution of GolgiPlug/Brefeldin A (BD Biosciences). Following surface marker staining (described below) cells were washed with Dulbecco's PBS then incubated with Ghost Dye UV450 (Tonbo) for live/dead discrimination. Cells were subsequently fixed with Cytofix/Cytoperm (BD Biosciences) following the manufacturer's recommended protocol. Intracellular staining was performed in the presence of BD Perm/Wash Buffer (BD Biosciences).

Flow cytometry on islet infiltrating T-cells was performed following the hand picking of islets from digested pancreata as previously described (21). The following modifications were performed in this study: following a second round of picking islets, instead of transferring islets into RPMI for overnight culture, islets were first picked into calcium and magnesium-free HBSS (Sigma-Aldrich; St. Louis, MO) supplemented with 0.5% Hyclone-FBS (ThermoFisher; Waltham, MA) and 2mM EDTA (ThermoFisher). These islets were then mechanically disrupted by vigorous pipetting and half the sample was dispersed for surface stain experiments while the other cells were used for *in vitro* cytokine experiments.

Fluorochrome labeled antibodies were obtained from the following vendors: Biolegend (San Diego, CA) - CD90.2 (30-H12, APC-Cy7), HLA-DQ (SK10, FITC), HLA-A,B,C (W6/32, APC-Cy7), H2-L^d/H2-D^b (28-14-8, PE), B220 (RA3–6B2, APC), H2-K^d (SF1.1, FITC), IFN-γ (XMG1.2; APC), TNF-α (MP6-XT22; PE-Cy7), CD357/GITR (DTA-1; PerCP-Cy5.5); BD Biosciences (Franklin Lakes, NJ) – Vβ8.1,2.3 (F23.1, FITC), TCRβ (H57–597, BV711), CD4 (GK1.5, BV785), CD4 (RM4–5; BV570), CD279/PD-1 (29F.1A12; BV711, CD25 (PC61; BV421); CD8α (53–6.7, BV480), CD45 (30-F11, BUV805), CD45.1 (A20, A700), H2-D^b (KH95, PE), I-A^d (AMS32.1 – cross reactive to H2-A^{g7}, PE), CD11b (M170, BV650), B220 (RA3–6B2, BUV496), CD90.2 (53–2.1, APC); Beckman Coulter (Pasadena, CA) – TCR-Vβ5.1 (IMMU 157, PE), TCR-Vβ22 (IMMU 546, FITC) IL-4 (11B11; PE), IL-5 (TRFK5; PE), IL-17A (TC11–18H10, BV786), CD69 (H1.2F3; BUV737); ThermoFisher Scientific: IL-13 (eBio13A; PE); Tonbo – CD11c (N418, redFluor 710).

Construction of NOD-cMHCI/II$^{-/-}$.DQ8, and NSG-cMHCI/II$^{-/-}$.DQ8 mice

NOD-*cMHCI/II*$^{-/-}$ and NSG.*Ab*^{0}.DQ8 mice (HLA-DQ8: *DQA*0301, DQB*0302)* were intercrossed and F1 hybrids were backcrossed to the NOD-*cMHCI/II*$^{-/-}$ parental strain. Backcross 1 (BC1) progeny carrying the desired combinations of edited genes and mutations were then selected for continued breeding. *Prkdc*^{scid}, *Il2rg*^{tm1Wjl}, Tg(HLA-DQA1), and Tg(HLA-DQB1) alleles were typed by JAX Transgenic Genotyping Service (JAX-TGS) using publicly available protocols. The *H2-Ab1*$^{b\text{-}tm1Doi}$ *(H2Ab*^{0}*)* mutation was made in 129S2/SvPas-derived stem cells and therefore is flanked by H2-K^b instead of the H2-K^d class I variant characterizing the NOD strain. 129S2/SvPas also carry H2-D^b, which is shared with NOD. Therefore, *H2-K1*$^{d\text{-}em1Dvs}$ *H2-Ab1*$^{g7\text{-}em1Dvs}$ *H2-D1*$^{b\text{-}em5Dvs}$ alleles were fixed by typing for H2-K^b and H2-D^b (which flank *H2-Ab1*) negative animals by flow cytometric analysis of blood mononuclear cells. Homozygosity of the *Prkdc*^{scid} mutation was additionally confirmed by typing for absence of $B220^+$ cells. Antibody against CD11b was used as a positive staining-control in mice lacking both B-lymphocytes and murine MHC expression. These efforts led to the generation of two new strains. The first is officially designated NOD.Cg-*H2-K1*$^{d\text{-}em1Dvs}$ *H2-Ab1*$^{g7\text{-}em1Dvs}$ *H2-D1*$^{b\text{-}em5Dvs}$ Tg(HLA-DQA1,HLA-DQB1)1Dv/Dvs, and throughout the rest of this study simply called NOD-*cMHCI/II*$^{-/-}$.DQ8 (where extra clarification is needed) or DQ8. The second is officially designated NOD.Cg-*Prkdc*^{scid} *H2-K1*$^{d\text{-}em1Dv}$*s H2-Ab1*$^{g7\text{-}em1Dv}$*s H2-D1*$^{b\text{-}em5Dvs}$ *Il2rg*^{tm1Wjl} Tg(HLA-DQA1,HLA-DQB1)1Dv/Dvs and hereafter in this study as NSG-*cMHCI/II*$^{-/-}$.DQ8.

NOD-cMHCI/II$^{-/-}$-A2

NOD-*cMHCI/II*$^{-/-}$ and NOD-*cMHCI*$^{-/-}$-A2 mice were intercrossed and resultant F1 hybrids backcrossed to the NOD-*cMHCI/II*$^{-/-}$ parental strain producing a new stock officially designated NOD/ShiLtDvs-*H2-K1*$^{d\text{-}em1Dvs}$ *H2-Ab1*$^{g7\text{-}em1Dvs}$ *H2-D1*$^{b\text{-}em5Dvs}$ Tg(HLA-A/H2-D/B2M)1Dvs/Dvs and hereafter in this study referred to as NOD-*cMHCI/II*$^{-/-}$-A2 (when additional clarification is needed) or simply A2. Mice were typed for the loss of H2-A^{g7} on B-lymphocytes by flow cytometry and eventual homozygosity of the Tg(HLA-A/H2-D/B2M)1Dvs transgene (following sister-brother mating NOD-*cMHCI/II*$^{-/-}$.A2$^{Tg/0}$ mice) via qPCR by JAX-TGS using a publicly available protocol.

NOD-cMHCI/II$^{-/-}$.DQ8-hTCR

The DQ8 restricted human TCR 20D11 recognizes Insulin $B_{9–23}$ and was derived from nPOD6323 T1D donor (22). The human 6H9 also recognizes Insulin $B_{9–23}$ in a DQ8 or DQ8-trans-restricted fashion and was isolated from nPOD6342 T1D donor (22). The A1.9 TCR recognizes human C-peptide$_{42–50}$ in a DQ8 restricted manner (23). The relevant human TCR alpha and beta variable antigen recognition sequences (Table I) have been fused to murine constant regions to create chimeric TCR genes. TCRα sequences have been inserted into vector pCD2, which drives expression from a human CD2 promoter (24). TCRβ sequences have been inserted into p428, which drives expression from a murine CD4 promoter (25). Plasmids were purified with an endotoxin-free kit (Nucleobond Xtra, Takara). Ten to fifteen micrograms of each plasmid were digested overnight with restriction enzymes (New England Biolabs) *Not*I (mCd4-TCRbeta) or *Not*I/*Sal*I (hCD2-TCRa) to remove the desired transgenic fragments from their plasmid backbones. Digested fragments were electrophoresed on a 1% GTG agarose gel (Lonza) and stained with crystal violet. Fragments of the desired size (Cd4-TCRbeta: 5.3 kb; CD2-TCRalpha: 12.4 kb) were excised and purified using a Nucleospin Gel & PCR fragment kit (Takara) according to the manufacturer's instructions and eluted in TE buffer (IDT) tested in-house to be non-toxic to murine embryos. Fragments were then mixed to an equimolar concentration, centrifuged at 20,000xg for 15 min, and the top 80% of the supernatant was removed to a clean microcentrifuge tube. Combined TCRa/TCRb DNA fragments were diluted to 2–3 ng/ul total DNA and injected into NOD-*cMHCI/II*$^{-/-}$ zygotes. Resulting transgenic founder mice were identified by PCR genotyping. Briefly, ear or tail samples were lysed in NaOH lysis buffer and neutralized by 40 mM TrisHCl. Each sample was subjected to three distinct genotyping assays to identify founder mice carrying both transgenes. Only founder mice positive in all three assays were used for establishing colonies. Assay1: TCRa PCR (9666–9668) amplifies an 1823 fragment encompassing the human CD2 promoter, TCRA, and the hCD2 locus control region. Assay2: TCRa PCR (9673–9671) amplifies the 3' end of the hCD2 locus control region. Assay3: TCRb PCR (9675–9681) amplifies a 1031 bp fragment from the mouse Cd4 intron1 to coding sequence of TCRbeta. Primers: 9666: GGCAAAGGAGCACATCAGAAGG, 9668: TGTTCGGGTCATTCTGGTGAGG, 9673: TCAGGATGTTTCCTCTCACCAC, 9671: TCCACTTCCCAGGTTCCAGC, 9675: TGGGTTGGTTATCAAGGTCCTG, 9681: CCACTGACCAGCACAGCATATAG. Identified founders were crossed with NOD-*cMHCI/II*$^{-/-}$.DQ8 mice. Resulting positive offspring were backcrossed to NOD-*cMHCI/II*$^{-/-}$.DQ8 mice two times for A1.9 and three times for 6H9 and 20D11. After intercrossing carriers of both TCR-α and TCR-β transgenes,

subsequent progeny were typed by the JAX-TGS to fix the TCR and HLA-DQ transgenes to homozygosity. qPCR primers and probes used by JAX-TGS to type these new hTCR transgenes are listed in Table II. The formal strain designations for the primary lines used in this manuscript are as follows: NOD-*cMHCI/II*$^{-/-}$.DQ8–20D11 (hereafter DQ8–20D11) [NOD.Cg-*H2-K1*$^{d\text{-}em1Dvs}$ *H2-Ab1*$^{g7\text{-}em1Dvs}$ *H2-D1*$^{b\text{-}em5Dvs}$ Tg(HLA-DQA1,HLA-DQB1)1Dv Tg(CD2-Tcra20D11,Cd4-Tcrb20D11)1Dvs/Dvs], NOD-*cMHCI/II*$^{-/-}$.DQ8–6H9 (hereafter DQ8–6H9) [NOD.Cg-*H2-K1*$^{d\text{-}em1Dvs}$ *H2-Ab1*$^{g7\text{-}em1Dvs}$ *H2-D1*$^{b\text{-}em5Dvs}$ Tg(HLA-DQA1,HLA-DQB1)1Dv Tg(CD2-Tcra6H9,Cd4-Tcrb6H9)2Dvs/Dvs], NOD-*cMHCI/II*$^{-/-}$.DQ8-A1.9 [NOD.Cg-*H2-K1*$^{d\text{-}em1Dvs}$ *H2-Ab1*$^{g7\text{-}em1Dvs}$ *H2-D1*$^{b\text{-}em5Dvs}$ Tg(HLA-DQA1,HLA-DQB1)1Dv Tg(CD2-TcraA1.9,Cd4-TcrbA1.9)1Dvs/Dvs].

NSG.*H2Ab*^{0}.DQ8.hINS were crossed to the NOD-*cMHCI/II*$^{-/-}$.DQ8 strain. Offspring hemizygous for Tg(INS*)172Dvs were continually backcrossed to NOD-*cMHCI/II*$^{-/-}$.DQ8 mice to remove the *Prkdc*^{scid}, *H2Ab*^{0} and *Il2rg*^{tm1Wjl} mutations. *Prkdc*^{scid}, *Il2rg*^{tm1Wjl} and Tg(INS*)172Dvs were typed by the JAX-TGS, while loss of the *H2Ab*^{0} mutation was typed by flow as described above. The Tg(INS*)172Dvs transgene was typed using the following primers (Forward: CTCAAATCGCACCCTTCTGT; Reverse: TAGAGAGGATCAGGGGATGC; Internal Positive Control Forward: CTAGGCCACAGAATTGAAAGATCT; Internal Reverse Control: GTAGGTGGAAATTCTAGCATCATCC). More details on this typing protocol are publicly available on the web page for JAX strain 026936. Resulting NOD-*cMHCI/II*$^{-/-}$.DQ8.hINS mice were crossed to the DQ8-A1.9 strain. TCR-hemizygous F1 females were entered into a T1D incidence study, while males were backcrossed to DQ8-A1.9 females to re-fix the TCR transgenes to homozygosity. After two generations of backcrossing to NOD-*cMHCI/II*$^{-/-}$.DQ8-A1.9, these strains are now maintained in a single colony through sister-brother matings of hINS^{hemi} x hINS^{-} mice. NOD.Cg-*H2-K1*$^{d\text{-}em1Dvs}$ *H2-Ab1*$^{g7\text{-}em1Dvs}$ *H2-D1*$^{b\text{-}em5Dvs}$ Tg(HLA-DQA1,HLA-DQB1)1Dv Tg(CD2-TcraA1.9,Cd4-TcrbA1.9)1Dvs Tg(INS*)172Dvs/Dvs (NOD-*cMHCI/II*$^{-/-}$.DQ8-A1.9.hINS are hereafter referred to as DQ8-A1.9.hINS while NOD-*cMHCI/II*$^{-/-}$.DQ8-A1.9 (hINS^{-} littermates) are referred to as DQ8-A1.9.

NOD.scid-cMHCI/II$^{-/-}$.DQ8–20D11

Male NSG-*cMHCI/II*$^{-/-}$.DQ8 mice were crossed to DQ8–20D11 mice. Male offspring of this cross were crossed a second time to DQ8–20D11. Mice homozygous for 20D11 transgenes, *Il2rg*$^{+/+}$, and carrying the *Prkdc*^{scid} mutation were intercrossed to fix the *Prkdc*^{scid} mutation back at homozygosity. These mice have been assigned the formal strain name NOD.Cg-*Prkdc*^{scid} *H2-K1*$^{d\text{-}em1Dvs}$ *H2-Ab1*$^{g7\text{-}em1Dvs}$ *H2-D1*$^{b\text{-}em5dvs}$ Tg(HLA-DQA1,HLA-DQB1)1Dv Tg(CD2-Tcra20D11,Cd4-Tcrb20D11)1Dvs/Dvs, (hereafter NOD.*scid*-*cMHCI/II*$^{-/-}$.DQ8–20D11).

NOD-cMHCI/II$^{-/-}$.DQ8-A2 and NOD-cMHCI/II$^{-/-}$.DQ8-A2–20D11

NOD-*cMHCI/II*$^{-/-}$-A2 and NOD-*cMHCI/II*$^{-/-}$.DQ8 mice were intercrossed to generate a NOD-*cMHCI/II*$^{-/-}$.DQ8-A2 strain (hereafter, DQ8-A2, formal strain NOD.Cg-*H2-K1*$^{d\text{-}em1Dvs}$ *H2-Ab1*$^{g7\text{-}em1Dvs}$ *H2-D1*$^{b\text{-}em5Dvs}$ Tg(HLA-A/H2-D/B2M)1Dvs Tg(HLA-DQA1,HLA-DQB1)1Dv/Dvs). DQ8–20D11 and DQ8-A2 mice were intercrossed to

generate a NOD-*cMHCI/II*$^{-/-}$.DQ8-A2–20D11 strain (hereafter DQ8-A2–20D11, formal strain name NOD.Cg-*H2-K1*$^{d\text{-}em1Dvs}$ *H2-Ab1*$^{g7\text{-}em1Dvs}$ *H2-D1*$^{b\text{-}em5Dvs}$ Tg(HLA-A/H2-D/B2M)1Dvs Tg(HLA-DQA1,HLA-DQB1)1Dv Tg(CD2-Tcra20D11,Cd4-Tcrb20D11)1Dvs/Dvs). For both strains, Tg(HLA-A/H2-D/B2M)1Dvs, Tg(HLA-DQA1,HLA-DQB1)1Dv, Tcra-20D11, and Tcrb-20D11 were all typed via qPCR by JAX-TGS and the colony is now maintained in a homozygous state for all mutations and transgenes.

Monitoring for T1D development

Mice were checked weekly for glucosuria using Ames Diastix (Bayer; Leverkusen, Germany). Mice were considered diabetic after two readings of >0.25% (corresponding to 300mg/dl in blood).

Insulitis

Pancreata were fixed in Bouins (Rowley Biochemical; Danvers, MA) and embedded in paraffin blocks. Three levels, separated at 100 μm, were sectioned and stained with H&E and aldehyde fuchsin. Mean insulitis scores (MIS) were calculated by a blinded observer as previously described (26, 27). As photographically documented in (27), this scoring system combines analysis of immune cell infiltrate (H&E), in conjunction with a quantitative determination of β-cell loss (as determined by loss of aldehyde fuchsin staining). Briefly, the scoring system for individual islets is as follows: 0, no lesions; 1, peri-insular aggregates; 2, <25% islet destruction; 3, >25% islet destruction; 4, >75% islet destruction. The final score was determined by dividing the summed score for each pancreas by the total number of islets examined. Representative insulitis histology image was obtained from slides scanned with a Hamamatsu NanoZoomer C9600–12 (Shizuoka, Japan). Image was exported from NDP.view2 as a *.jpg file and a greyscale filter (Red 0.6, Green 0.2, Blue 0.1, Lightness 0) applied in Inkscape 1.2.

Myocarditis Assessment

Myocarditis severity was assessed on 4 areas (left ventricular free wall, septum, anterior and posterior left ventricle) of H&E-stained midline cross-sections of the heart for a semi-quantitative score. Scoring was performed as follows; 0, healthy myocardial morphology; 1, mild infiltration observed as an increase in mononuclear cells between cardiomyocyte fibers; 2, moderate infiltration with small inflammatory lesions mostly restricted to the epicardial area; 3, severe inflammatory lesions throughout the myocardium. Scores from the 4 evaluated cardiac areas in each mouse were then summed. Representative images were obtained from stained slides (H&E or Sirius Red) scanned with a Hamamatsu NanoZoomer C13239–01 (Shizuoka, Japan). Images were exported from NDP.view2 as a *.jpg file.

Transfer Experiments

Single cell suspensions of splenocytes were prepared as described above in HBSS supplemented with 2% FBS from individual DQ8–20D11 mice (Line 1) or from a now extinct Line 4 cohort. Cells were resuspended in dPBS with calcium and magnesium (ThermoFisher Scientific) and 10×10^6 total splenocytes were transferred via tail vein injection into NSG-*cMHCI/II*$^{-/-}$.DQ8 recipients. Cells from a total of two females and

two males from each line was injected into 3–5 sex matched recipients. Recipients were monitored for T1D development for up to 30 weeks.

qPCR

Spleens were harvested from ten- to fifteen-week-old female mice and RBC-depleted single cell suspensions were prepared as above. $CD4^+$ T-cells were negatively enriched over LD columns (Miltenyi Biotec; North Rhine-Westphalia, Germany) after incubation with biotinylated antibodies directed against B220, Ter119, CD11c, CD11b, and CD8 and incubation with Streptavidin MicroBeads (Miltenyi Biotec). Enriched $CD4^+$ T-cells were frozen in 1mL Trizol (Thermo Fisher Scientific, Waltham, MA) at −80°C. Total RNA was then prepared by phenol-chloroform extraction and reverse transcribed (SuperScript IV VILO Master Mix, Thermo Fisher Scientific) following manufacturer's methods. qPCR was performed using Power SYBR Green PCR Master Mix (Applied Biosystems, Thermo Fisher Scientific) on a QuantStudio 7 Flex real time PCR system (Applied Biosystems). Transgenic hTCR gene expression was normalized to CD90 gene expression in the sample (to normalize to T-cell count) and compared across the relevant mouse strains. Primers were as follows: *20D11 Tcra* (F: 5'-GAAGGTTTACAGCACAGGTCG-3'; R: 5'-CACCAGAAAGAATTGCACAGAGG-3'); *20D11 Tcrb* (F: 5'-GAAGATCCGGTCCACAAAGC-3'; R: 5'-ATGGCTCAAACAAGGAGACC-3'); *6H9 Tcra* (F: 5'-ACCAATGAAATGGCCTCTCTG-3'; R: 5'-TCGACTCTGACGATGCAATAG-3'); *6H9 Tcrb* (F: 5'-TCTCCCAGTCCCCCAGTAAC-3'; R: 5'-GCCTCTGTCGGTACCAGTAA-3'); *A1.9 Tcra* (F: 5'-GACTCGCTTTTGGGAAGGGG-3'; R: 5'-AGTCAAAGTCGGTGAACAGGC-3'); *A1.9 Tcrb* (F: 5'-GGCTACACCTTCGGTTCGG-3'; R: 5'-TGCAATCTCTGCTTTTGATGGC-3'); *CD90* (F: 5'-ACCAAGGATGAGGGCGACTA-3'; R: TCTGAACCAGCAGGCTTATG-3').

Insulin Secretion Assay

Briefly, mice were fasted for 5 hours and injected with glucose (2g/kg body weight, intraperitoneally). Blood samples (~20 μl) were collected from tail tip using Microvette tubes, (Sarstedt Inc, Germany) at 0, 15, 30, 60 and 120 minutes for insulin measurements. Plasma was separated and insulin levels were quantified using Ultra-sensitive mouse-insulin ELISA kits as per the manufacturer's guidelines (CrystalChem, IL, USA).

Statistics

All statistics are calculated using Prism 9. Scatter dot plots display biological replicates and mean ± standard deviation. Biological replicates are combined from a minimum of two independent experiments. P-values are calculated with two-tailed Mann-Whitney analyses for two group comparisons and one-way ANOVA with Tukey's multiple comparisons test for more than two groups.

Results

Creation of NOD-cMHCI/II$^{-/-}$-A2 and NOD-cMHCI/II$^{-/-}$-DQ8 mice

In an effort to further refine our "HLA-humanized" NOD mouse models (7), we introduced, through genetic crossing, transgenic constructs encoding T1D relevant *HLA-A*02:01* (HLA-A2) or *HLA-DQA*0301,DQB*0302)* (HLA-DQ8) molecules into our previously described NOD-*cMHCI/II*$^{-/-}$ mice (7). Resulting murine MHC bare A2 and DQ8 mice express human MHC I or II molecules while being devoid of classical murine MHC I and II (Figure 1A). As expected, A2 mice generate predominantly CD8$^+$ T-cells, while DQ8 mice produce mostly CD4$^+$ T-cells (Figure 1B). As has been reported for other NOD strains carrying HLA-DQ8 transgenes, our new NOD-*cMHCI/II*$^{-/-}$.DQ8 mice do develop myocarditis with cellular infiltration and fibrosis (Supplemental Figure 1A, B). While this phenotype is under active investigation, it is outside the scope of this current manuscript.

Creation of NOD-cMHCI/II$^{-/-}$.DQ8–20D11

Plasmids containing chimeric murine-constant-region human-variable region TCR sequences from the T1D patient derived T-cell clone 20D11 (Table I) were injected into *NOD-cMHCI/II*$^{-/-}$ zygotes and resultant founder mice crossed to the NOD-*cMHCI/II*$^{-/-}$.DQ8 strain. 20D11 T-cells recognize insulin $B_{9–23}$ (22), an epitope shared between mouse and humans. Four initial lines were generated. While in the process of fixing the relevant HLA-DQ8 and hTCR transgenes to a homozygous status, a preliminary experiment was performed using two lines of mice (Line 1 and Line 4) that were the first to be HLA-DQ8 homozygous, but still hTCR hemizygous. During the creation of NOD-*cMHCI/II*$^{-/-}$.DQ8 mice, we simultaneously developed a NSG-*cMHCI/II*$^{-/-}$.DQ8 strain (Supplemental Figure 2) for use as immunodeficient recipients for transfer studies. Therefore, to test functionality of the 20D11 T-cells 10×10^6 whole splenocytes from either NOD-*cMHCI/II*$^{-/-}$.DQ8 Line 1 or Line 4 20D11 donors were transferred into NSG-*cMHCI/II*$^{-/-}$.DQ8 recipients. While no resulting recipients developed overt T1D, those engrafted with DQ8–20D11 Line 1 splenocytes had higher levels of insulitis indicating the transgenic hTCR is functionally active (Figure 2A). These data, along with an apparent reduced transgenic Vβ usage for Line 4 (data not shown), lead to the decision to prioritize Line 1 for further studies. From this point forward, DQ8–20D11 refers to Line 1.

Compared to DQ8 controls DQ8–20D11 mice have a slightly reduced percentage of CD90$^+$ T-cells amongst CD45$^+$ splenocytes (Figure 2B). Additionally, there is a slight reduction in the percentage of CD4$^+$ amongst CD90$^+$ cells in DQ8–20D11 mice (Figure 2C), possibly indicating negative selection pressure on transgenic TCR expressing cells. This is not at the expense of CD8$^+$ cells however, but rather there is an expansion of a CD4$^-$CD8$^-$ (DN) fraction (Figure 2C). Compared to DQ8 mice which lack hTCR transgenes, a vast majority of DQ8–20D11 CD4 cells express the transgenic Vβ22 (Figure 2D). Around 50% of DN T-cells express the transgenic Vβ22 (Figure 2E). Finally, enriched T-cells were confirmed to express the transgenic TCRα and TCRβ mRNA by qPCR (Figure 2F).

Creation of NOD-cMHCI/II$^{-/-}$.DQ8–6H9 mice

The 6H9 hTCR also recognizes insulin $B_{9–23}$ (22). As we did for 20D11, plasmids containing the chimeric hTCR sequences (Table I) for 6H9 were injected into NOD-*cMHCI/II*$^{-/-}$ zygotes and resultant founders crossed to the NOD-*cMHCI/II*$^{-/-}$.DQ8 strain, initially generating two transgenic lines. Subsequent breeding issues (and lack of any insulitis development, Supplemental Figure 3) for 6H9 Line 1 led us to focus on DQ8–6H9 Line 2 mice. No differences in CD90 percentage amongst CD45 (Figure 3A) or CD4 vs CD8 percentage amongst T-cells (Figure 3B) were observed between DQ8–6H9 and DQ8 control mice. The 6H9 TCRα and TCRβ transgenic mRNAs are both expressed (Figure 3C).

hTCR transgenic T-cells recognizing insulin $B_{9–23}$ induce insulitis in NOD-cMHCI/II$^{-/-}$.DQ8 mice

We have yet to observe overt T1D in DQ8 (0/20), DQ8–20D11 (0/19, 4 sick non-diabetic mice) or DQ8–6H9 mice (0/21) out to 30-weeks-of-age. Therefore, we histologically examined pancreata to determine whether we could detect differences in insulitis progression between the various strains. At 10–15 weeks of age, both DQ8–20D11 and DQ8–6H9 mice have higher levels of insulitis compared to the DQ8 control strain (Figure 4A). At this age DQ8–20D11 mice have higher levels of insulitis than the DQ8–6H9 stock. However, by 30 weeks of age, insulitis in the DQ8–6H9 strain equalized to that in DQ8–20D11 mice. Both strains had increased insulitis compared to DQ8 controls without transgenic TCRs at each examined age (Figure 4B). A second line of 20D11 with similar levels of insulitis as Line 1 (Supplemental Figure 3) is backed up as frozen sperm. While these mice remain normoglycemic, the dynamics of the metabolic response differ, as measured by insulin secretion after glucose challenge; both the DQ8–20D11 and DQ8–6H9 strains were lower compared to parental DQ8 mice (Figure 4C). Combined, these data indicate that both 20D11 and 6H9 transgenic T-cells selected in a HLA-“humanized” murine thymus are both functional as indicated by an ability to mediate spontaneous insulitis, although each TCR does so with differing kinetics.

We wondered why there may be differing kinetics in insulitis between the two strains. While the 6H9 TCR β-chain is expressed (Figure 3C), we were unable to determine the amount of protein on the cell surface due to a lack of a viable staining antibody. Therefore, we checked for evidence of allelic exclusion in both 20D11 and 6H9. To our surprise, we found there was no difference in murine Vβ8 expression between 6H9 and DQ8 mice (Figure 4D, E). However, 20D11 lacked murine Vβ8 (Figure 4D, E). These data indicate that the 20D11, but not the 6H9 TCR β-chain signals strongly enough to induce allelic exclusion.

Since 20D11, but not 6H9 exhibited a drop in percentage of both CD90$^+$ T-cells and those within the CD4$^+$subset, we wondered whether negative selection was occurring in the former strain. Therefore, we developed a NOD.*scid*-*cMHCI/II*$^{-/-}$.DQ8–20D11 strain to prevent the development of any endogenous TCR expressing cells. Compared to NSG-*cMHCI/II*$^{-/-}$.DQ8 mice, the NOD.*scid*-*cMHCI/II*$^{-/-}$.DQ8–20D11 strain did develop CD90$^+$ TCRβ$^+$ T-cells. This indicated 20D11 transgenic T-cells are positively selected in the absence of endogenous murine TCR chains (Figure 4F). However, compared to standard 20D11 mice, the percentage of CD4$^+$ 20D11 T-cells is drastically reduced in the *scid* carrying

stock suggesting the transgenic TCR does undergo some level of negative selection (Figure 4G). In comparison, the percentages of $CD8^+$ and DN T-cells are increased in NOD.*scid-cMHCI/II*$^{-/-}$.DQ8–20D11 mice (Figure 4G). This change in the T-cell compartment is due to the loss of $CD4^+$ T-cells, and not a numerical expansion of $CD8^+$ or DN T-cells, as the yield of $CD4^+$ T-cells is reduced nearly 10-fold (Figure 4H). Conversely, the yield of $CD8^+$ T-cells in NOD.*scid-cMHCI/II−/−.DQ8*-20D11 compared to DQ8–20D11 mice is not different, while the numbers of DN T-cells is slightly reduced (Figure 4H). Despite evidence of negative selection occurring with forced restriction of the transgenic TCRαβ pairing, the T-cells that survive to the periphery in NOD.*scid-cMHCI/II*$^{-/-}$.DQ8–20D11 are still capable of causing insulitis by 20-weeks-of-age (Figure 4I), with the occasional individual islets showing near complete destruction (labelled in the figure with a corresponding score of 4).

Next, we asked if we could detect any further differences that distinguished 20D11 and 6H9 T-cells. At 15–18 weeks of age, islet derived 20D11 T-cells have an increased TCR MFI compared to those from both NOD and 6H9 mice (Figure 5A). Both 20D11 and 6H9 $CD4^+$ T-cells show higher levels of $CD69^-$ PD-1^+ surface markers than standard NOD $CD4^+$ T-cells (Figure 5B, C). 20D11 T-cells exhibit higher levels than 6H9 at this same period. This data indicates past antigen exposure and activation has already occurred on ~10–15% of transgenic T-cells in the spleen. Furthermore, 20D11 T-cells also exhibit a slight elevation in $CD69^+$ PD-1^+ cells, indicating more recent activation events (Figure 5B, C). Interestingly, while no differences were observed on intra-islet infiltrating 6H9 T-cells compared to NOD controls, those from the 20D11 strain had a reduced level of those with a $CD69^-$ PD-1^+ phenotype, but with increases in both the $CD69^+$ PD-1^+ and $CD69^+$ PD-1^- fractions (Figure 5B, D). Together, these data indicate 20D11 T-cells are actively being stimulated by antigen ($CD69^+$) but are also prone to tolerance induction (PD-1^+) following activation.

Next, we looked for levels of Treg between the three strains. In spleens, $CD25^+$ $GITR^+$ Tregs were slightly reduced in 6H9 mice, compared to the 20D11 and NOD strains (Figure 5E, F). Interestingly, proportions of both $CD25^+$ $GITR^+$ and $CD25^-$ $GITR^+$ cells were increased among 20D11 T-cells. In the islets, Tregs ($CD25^+$, $GITR^+$) were slightly expanded in 20D11 mice compared to the 6H9 and NOD strains (Figure 5E, G). All three stains display high, but non-differing, levels of $GITR^+$ non-Tregs ($CD25^-$) (Figure 5G). Since GITR is upregulated on non-Tregs following TCR stimulation (28), these data provide further evidence of 20D11's antigenic activation *in vivo*, as well as indicating a potential increase in the ability of these cells to become Tregs.

We next examined consequences of *ex-vivo* re-stimulation of these hTCR T-cells. Immediately following cellular isolation, single cell suspensions from spleens or islets were re-stimulated *ex vivo* with PMA and ionomycin for four hours. Following re-stimulation, we observed little difference in splenic T-cell TNF-α or IFN-γ production between NOD, 6H9, or 20D11 total T-cells (Figure 5H, I). Intriguingly, there was a slight reduction in TNF-α and a large decrease in IFN-γ production by islet infiltrating 20D11 T-cells (Figure 5J, K). Very little IL-4,5,13 or IL-17A was detectable in any sample (data not shown). Taken together, these data indicate that despite signs of T-cell activation, 20D11 T-cells appear to have taken on a tolerized phenotype, likely due to high induction of PD-1 expression.

Creation of NOD-cMHCI/II$^{-/-}$.DQ8-A1.9 mice +/− human insulin

A1.9 is a human T-cell clone isolated from the pancreatic islets of a deceased T1D organ donor that recognizes human C-peptide$_{42–50}$ and only weakly cross reacts with murine proinsulin (23). Plasmids containing the chimeric A1.9 hTCR (Table I) were injected into NOD-*cMHCI/II*$^{-/-}$ zygotes and resulting founders were crossed to NOD-*cMHCI/II*$^{-/-}$.DQ8 mice. Four initial founders were quickly reduced to two lines (one line was lost to lack of germline transmission, whereas another appeared to have a Y-chromosome integration). Due to breeding difficulties with Line 2, all experimentation has been done with Line 1. While developing DQ8-A1.9, we separately generated, through genetic crossing, NOD-*cMHCI/II*$^{-/-}$.DQ8 mice carrying the human derived Tg(INS*)172Dvs transgene characterized by a 26–63 ACAGGGGTGTGGGG class I variable number of tandem repeat element (hINS) linked to T1D susceptibility (29). In order to test the functionality of the A1.9 T-cell in the presence or absence of hINS, we intercrossed DQ8-A1.9 and NOD-*cMHCI/II*$^{-/-}$.DQ8.hINS^{hemi} strains resulting in NOD-*cMHCI/II*$^{-/-}$.DQ8.hINS mice. F1 females which were either A1.9^{hemi} hINS^{hemi} or A1.9^{hemi} hINS^{-} were entered into a T1D incidence study. Males (positive for hINS) were backcrossed to the DQ8-A1.9 strain to refix the A1.9 transgenes to homozygosity. While neither A1.9^{hemi} hINS^{hemi} nor A1.9^{hemi} hINS^{-} females developed overt T1D (0/18, 1 sick nondiabetic vs 0/15, 3 sick nondiabetic) we observed that insulitis levels were higher in A1.9^{hemi} hINS^{hemi} than A1.9^{hemi} hINS^{-} females (Figure 6A).

After fixing the A1.9 transgenes back to homozygosity, we examined 10–15-week-old DQ8-A1.9 mice positive or negative for the hINS transgene for T-cell development. Mice hemizygous for the hINS transgene had a slightly reduced %CD90^{+} amongst splenic CD45^{+} cells (Figure 6B). There was also a minor, but significant reduction in the frequency of CD4^{+} cells amongst CD90^{+} T-cells (Figure 6C). These results indicate that in the presence of hINS, A1.9 expressing T cells may be under increased negative selection pressure. Enriched splenic T-cells from both DQ8-A1.9 and DQ8-A1.9.hINS mice expressed the transgenic Vβ5.1 while DQ8 mice did not (Figure 6D,E). Both strains also showed expression of both transgenic A1.9 Vα and Vβ mRNA as assayed by qPCR (Figure 6F). At this 10–15-week timepoint, DQ8-A1.9.hINS mice already have increased insulitis compared to DQ8-A1.9 littermates (Figure 6G).

Creation of NOD-*cMHCI/II*$^{-/-}$*.DQ8-A2 and* NOD-*cMHCI/II*$^{-/-}$*.DQ8-A2–20D11 mice*

We reasoned one explanation for the lack of overt T1D in the hTCR mice discussed to this point could be the lack of endogenous CD8^{+} T-cells selected by “classical” MHC I molecules. Therefore, to create a platform that could be used to introduce both CD4 and CD8 hTCR transgenes, we intercrossed NOD-*cMHCI/II*$^{-/-}$-A2 and NOD-*cMHCI/II*$^{-/-}$.DQ8 mice to generate a new DQ8-A2 strain. DQ8-A2 mice express both HLA-DQ8 and HLA-A2 (Figure 7A, B) while lacking classical murine MHC molecules (Figure 7B, C). This allows the selection of both CD4^{+} and CD8^{+} T-cells that are human HLA-DQ8 or HLA-A2 restricted (Figure 7E, F, G, H).

An intercross of *DQ8-A2* and DQ8–20D11mice generated a DQ8-A2–20D11strain. F1 females from this cross (hemizygous for both HLA-A2 and 20D11) were entered into a T1D incidence study. Males were used to begin the process of fixing the HLA-A2 and

20D11 transgenes. We have observed no diabetes for any A2 (0/20, with 5 sick nondiabetic), DQ8-A2 (0/28 from combined from two studies, 13 sick nondiabetic), or DQ8-A2–20D11 (0/23, 4 mice sick nondiabetic) mice. T1D did develop in a group of standard NOD controls analyzed concurrently with some of the above cohorts (16/25). Due to the large number of DQ8-A2 mice that were sick but not diabetic, we pathologically examined surviving mice, and as with the DQ8 model, observed myocarditis in DQ8-A2 mice lacking any of our human TCR transgenes (Supplemental Figure 1C, D,E). Despite the lack of overt T1D, DQ8-A2–20D11 mice had increased insulitis compared to either A2 or DQ8-A2 mice (Figure 7H), and lacked myocarditis found in either DQ8 or DQ8-A2 mice (Supplemental Figure 1E). Insulitis was, however, reduced in comparison to surviving NOD controls (Figure 7H).

Discussion

Herein we report the creation of ten new NOD-based “humanized” mouse models carrying varying combinations of T1D-associated HLA Class I and II alleles along with patient derived TCR-transgenes (Table III). Together these models could prove useful platforms for the future testing of potential interventions that aim to prevent pancreatic infiltration of diabetogenic T-cells. Despite the lack of overt T1D, through measurements of β-cells loss (histological methods that assess β-cells surface area/staining or functionally and assays such as insulin secretion) interventions can still be quantifiably tested in these HLA/TCR humanized NOD mice for efficacy. We should also note, islets with scores of 3 and 4 (as depicted in Figure 4I) were also quite large. NOD background mice are known to form “mega-islets” which is caused by a combination of strain-specific β-cell hyperactivity and lymphocyte infiltration (30, 31). This β-cell hyperactivity is likely the reason that even pre-diabetic standard NOD mice have normal levels of pancreatic insulin content until around 14 weeks of age (precipice where most NOD colonies start to have high penetrance of T1D) (32). Therefore, it is unsurprising we did not observe greater signs of β-cell dysfunction.

While we did attempt to combine HLA-DQ8 with HLA-B39, we were unable to maintain a viable NOD-*cMHCI/II*$^{-/-}$.DQ8-B39 colony despite our best efforts to breed mice in various combinations of homo- and heterozygosity due to rapid onset of non-T1D illness which in hindsight, was likely accelerated myocarditis. This indicates that certain HLA-pairings may be more feasible than others when using the NOD-*cMHCI/II*$^{-/-}$ platform to generate new combinations. DQ8 and DQ8-A2 mice were found to develop myocarditis, but minimal levels of insulitis (Figure 7H; Supplemental Figure 1A–D). In both strains, expression of the human 20D11 and A1.9 hTCR transgenes enhanced insulitis levels (Figure 4A,B; Figure 6A,G; Figure 7H), while reducing myocarditis development (Supplemental Figure 1E). Introduction of the 6H9 transgenic TCR also enhanced insulitis development in DQ8 mice (Figure 4A). However, the inability of the transgenic 6H9 TCR to induce allelic exclusion of endogenous TCRβ chain expression (Figure 4B) correlates with its failure to limit myocarditis development in DQ8 mice (Supplemental Figure 1 E).

We should note, due to the inability of the transgenic 6H9 TCR to induce allelic exclusion of endogenous murine TCRβ-chains, and the lack of an available specific-Vβ antibody to test its expression, we cannot rule out the following two possibilities. The first is the 6H9

transgenic β-chain is not capable of allowing for positive selection signals. Alternatively, the 6H9 transgenic β-chain *protein* is simply lowly (or not) expressed on the cell surface. Thus, future development of a 6H9 line carrying the *Prkdc*^{scid} mutation is warranted. If the 6H9 TCRβ-chain *protein* is not present on the surface, this would indicate expression of the human TCRα-chain paired with endogenous murine TCRβ-chains is sufficient to rescue insulitis development in DQ8 mice. We attempted to test several tetramers that may detect 20D11 and 6H9 T-cells in our newly developed mouse models. However, we were not able to find any optimal staining conditions. This could be due to the fact that these mice retain expression of murine CD4 molecules which may change the stability of TCR:MHC (tetramer) interactions.

The 20D11 and 6H9 TCRs recognize the shared human and murine $InsB_{9–23}$ epitope (22), and when expressed in 5KC cell lines exerted similar levels of reactivity to insulin (22). However, 20D11 and 6H9 expressing T-cells developing in our NOD based mouse models appear to have different affinities towards their cognate antigen. Several pieces of evidence point to this. First, DQ8–20D11 mice develop insulitis at a much earlier age than those expressing 6H9. Second, the slight reduction in peripheral $CD4^+$ cells amongst $CD90^+$ cells observed in 20D11 mice compared to the 6H9 model may indicate the former population is under greater thymic negative selection pressure. This is further supported by the enhanced reduction of $CD4^+$ T-cells when 20D11 is paired with the *Prkdc*^{scid} mutation. Additionally, islet infiltrating 6H9 T-cells more closely resemble those in standard NOD mice than 20D11 T-cells. 20D11 T-cells show a more antigen experienced, but exhausted or anergized, phenotype. Together, these pieces of evidence indicate the two T-cell clones may have different affinity or avidities towards their shared cognate antigen. Additional work dissecting TCR signaling after these TCRs encounter antigen are warranted. Preliminary analysis however reveals that 20D11 T-cells show earlier (or stronger) evidence of antigen stimulation as those in the spleen already show signs of CD69, PD-1, and GITR upregulation compared to standard NOD T-cells. Additionally, the same CD4 frequency reductions are also observed when A1.9 is paired with its cognate antigen, human pre-pro-insulin. Therefore, all of these models may have additional utility for studying signaling events and thymic selection of T-cells expressing varying human derived diabetogenic TCRs.

The functional nature and mechanisms of development of the expanded DN population observed in 20D11 mice should be pursued in future work. Whether this is a consequence of hypothesized negative selection pressures in the thymus is currently unknown. However, the expanded DN population is reminiscent to the expanded DN population observed for BDC2.5 TCR transgenic thymocytes in B6.*H2*^{g7} mice where these cells take on a TCRγδ transcriptomic profile (33). However, unlike the situation for BDC2.5, the 20D11 TCRβ is driven by the CD4 promoter, meaning expression likely begins properly during the thymic $CD4^+$ $CD8^+$ stage, and not at an earlier DN stage as might be the case for BDC2.5. The NOD.*scid*-*cMHCI/II*$^{-/-}$.DQ8–20D11 model will be useful in dissecting the functionality and nature of these DN T-cells.

We originally anticipated that NOD-*cMHCI/II*$^{-/-}$ mice expressing DQ8 and A2 alone were unlikely to develop insulitis, but those carrying both of these genes might do so. This

did not occur. However, introduction of hTCR transgenes derived from the 20D11 $CD4^+$ T-cell clone induced insulitis development in NOD-*cMHCI/II*$^{-/-}$.DQ8-A2 mice. While there are murine TCR transgenics that can develop overt T1D in the absence of $CD8^+$ T-cells (34), others require additional genetic modifications to induce spontaneous disease (35). Future work will aim to combine human diabetogenic $CD8^+$ T-cell (36) clone-derived TCR transgenes with those of $CD4^+$ T-cell origin described herein. Importantly, creation of the DQ8-A2 combination together with the hINS transgene would enable introduction of other hTCR transgenes, similar to A1.9, which respond to insulin epitopes unique to human insulin. Pairing of A1.9 with a CD8 clone, such as 1.C8 (which would also require pairing with the hINS transgene) (36) is warranted. Additionally, combination of A1.9 or 6H9 hTCR transgenes with the *Prkdc*^{scid} mutation, as we did for 20D11, would be of interest. This will remove potential issues with incomplete TCR allelic exclusion (37) interfering with overt T1D development.

Another recent report combined diabetogenic hTCRs with HLA-DR4 in NOD mice. This system (Hu-Rg) utilized a retrogenic approach to express patient derived GAD-reactive TCRs (38) in the base model NOD.HLA-DR4 Tg.*H2Ab1*$^{-/-}$.*Rag1*$^{-/-}$ mice. Unlike the 20D11, 6H9, and A1.9.hINS models described here, the Hu-Rg system required peptide pulsed DC priming to initiate *insulitis development* caused by the human TCRs. Whether this would be necessary for all TCR combinations is unknown. Based on our observations with 20D11 and 6H9 it is likely that different TCRs may not require priming to initiate *insulitis* when expressed within that system. We did not test whether antigen priming could precipitate insulitis development for the “non-functional” lines tested in this work (Supplementary Figure 3). Interestingly, NOD.HLA-DR4 Tg.*H2Ab1*$^{-/-}$ mice themselves had age-related insulitis development in the absence of the human TCR retrogenes (38). This also contrasts with our models, which do not develop significant insulitis in the absence of hTCR transgenes. We have two possible explanations for this discrepancy. First, it is possible HLA-DR4 has a greater capacity than the DQ8 variant to select insulitis causative murine T-cells. In this scenario, we may consider humanization of the CD4 molecule in our system which may improve the ability of HLA-DQ8 to select T-cells that cause insulitis and not myocarditis (39–41). In our HLA-A2 system, murine CD8 interactions with the MHC are maintained, due to the chimeric HHD molecule retaining a murine constant region (42). In contrast, the HLA-DQ8 α- and β-chain transgenes utilized here are not similarly optimized for interactions with murine CD4. Alternatively, the complete humanization of both MHC I and MHC II in our model is contributing to the lack of insulitis development. While we have previously observed that HLA-A2 can select $CD8^+$ T-cells that cause T1D, it did so in the presence of NOD H2-$A2^{g7}$ MHC II variant (7). Therefore, it is reasonable to assume that $CD4^+$ T-cell populations required to provide help to HLA-A2 selected $CD8^+$ T-cells are missing when HLA-DQ8 is used as the MHC II molecule. The future introduction of HLA-DR4 paired with HLA-A2 in our model system is warranted to test whether this applies to other human MHC II molecules.

Supplementary Material

Refer to Web version on PubMed Central for supplementary material.

Acknowledgements

The authors would like to thank The Jackson Laboratory's Genetic Engineering Technologies, Flow Cytometry Core, Histopathology Services, Microscopy Core, and Transgenic Genotyping Services for technical support. We also gratefully acknowledge the contribution of Dr. Ansarullah from the Metabolic Phenotyping Service (Center for Biometric Analysis) at The Jackson Laboratory for his expert assistance. Finally, the authors are grateful for the support of Carl Stiewe and his wife, Maike Rohde, whose generous donation toward T1D research at The Jackson Laboratory has contributed to the development of these new mouse models.

JJR was supported during parts of this work by JDRF Fellowship 3-PDF-2017-372-A-N and DRC 27 P20–0201 JR. AM was supported by an Institutional Development Award (IDeA) from the National Institute of General Medical Sciences of the National Institutes of Health under grant number P20GM103423 (via Maine IDeA Network of Biomedical Research Excellence). JRD was supported during parts of this work by Diabetes Research Connection grant DRC 43 P21–0334. This work made use of a previously unpublished mouse model developed by the Type 1 Diabetes Resource (NIH 1UC4DK097610-01, DVS). MN was additionally supported by NIH grants R01DK133457 and P30DK116073. CE and SM were supported by The National Health and Medical Research Council (NHMRC GNT1123586). DVS was supported by NIH grants DK-95735 and U54OD020351, JDRF grant 2-SRA-2018-568-S-B (DVS, MN, SM), and Mark Foundation MFCR ASPIRE Serreze FY22. This work was also partly supported by U54OD030187 and Cancer Center Support Grant CA034196.

JJR designed and conducted experiments, analyzed data, and wrote the manuscript. AM conducted experiments. JRD conducted experiments. RM conducted experiments to prepare transgenic constructs for microinjection and identified founder mice. OB processed hearts for histology. EF and SS examined and scored heart histology to confirm myocarditis development. LL and CE generated the transgenic constructs used in this study. AP provided the human Tg(INS*)172 transgene construct. MN, SM, and DVS contributed to study conception. MN and SM contributed to writing of the manuscript. NR supervised experimental efforts for heart histology and scoring. DVS supervised experimental effort, scored pancreata histology, and supervised writing of the manuscript.

References

1. Atkinson MA, and Leiter EH. 1999. The NOD mouse model of type 1 diabetes: as good as it gets? Nat Med 5: 601–604. [PubMed: 10371488]
2. Jarchum I, Baker JC, Yamada T, Takaki T, Marron MP, Serreze DV, and DiLorenzo TP. 2007. In vivo cytotoxicity of insulin-specific CD8+ T-cells in HLA-A*0201 transgenic NOD mice. Diabetes 56: 2551–2560. [PubMed: 17620420]
3. Marron MP, Graser RT, Chapman HD, and Serreze DV. 2002. Functional evidence for the mediation of diabetogenic T cell responses by HLA-A2.1 MHC class I molecules through transgenic expression in NOD mice. Proceedings of the National Academy of Sciences of the United States of America 99: 13753–13758. [PubMed: 12361980]
4. Niens M, Grier AE, Marron M, Kay TW, Greiner DL, and Serreze DV. 2011. Prevention of "Humanized" diabetogenic CD8 T-cell responses in HLA-transgenic NOD mice by a multipeptide coupled-cell approach. Diabetes 60: 1229–1236. [PubMed: 21346176]
5. Takaki T, Marron MP, Mathews CE, Guttmann ST, Bottino R, Trucco M, DiLorenzo TP, and Serreze DV. 2006. HLA-A*0201-restricted T cells from humanized NOD mice recognize autoantigens of potential clinical relevance to type 1 diabetes. J Immunol 176: 3257–3265. [PubMed: 16493087]
6. Unger WW, Pearson T, Abreu JR, Laban S, van der Slik AR, der Kracht SM, Kester MG, Serreze DV, Shultz LD, Griffioen M, Drijfhout JW, Greiner DL, and Roep BO. 2012. Islet-specific CTL cloned from a type 1 diabetes patient cause beta-cell destruction after engraftment into HLA-A2 transgenic NOD/scid/IL2RG null mice. PLoS One 7: e49213. [PubMed: 23155466]
7. Racine JJ, Stewart I, Ratiu J, Christianson G, Lowell E, Helm K, Allocco J, Maser RS, Chen YG, Lutz CM, Roopenian D, Schloss J, DiLorenzo TP, and Serreze DV. 2018. Improved Murine MHC-Deficient HLA Transgenic NOD Mouse Models for Type 1 Diabetes Therapy Development. Diabetes 67: 923–935. [PubMed: 29472249]
8. Roopenian DC, and Akilesh S. 2007. FcRn: the neonatal Fc receptor comes of age. Nat Rev Immunol 7: 715–725. [PubMed: 17703228]
9. Roopenian DC, Christianson GJ, Sproule TJ, Brown AC, Akilesh S, Jung N, Petkova S, Avanessian L, Choi EY, Shaffer DJ, Eden PA, and Anderson CL. 2003. The MHC class I-like IgG receptor controls perinatal IgG transport, IgG homeostasis, and fate of IgG-Fc-coupled drugs. J Immunol 170: 3528–3533. [PubMed: 12646614]

10. Baker K, Rath T, Pyzik M, and Blumberg RS. 2014. The Role of FcRn in Antigen Presentation. Frontiers in immunology 5: 408. [PubMed: 25221553]
11. Chaudhury C, Mehnaz S, Robinson JM, Hayton WL, Pearl DK, Roopenian DC, and Anderson CL. 2003. The major histocompatibility complex-related Fc receptor for IgG (FcRn) binds albumin and prolongs its lifespan. The Journal of experimental medicine 197: 315–322. [PubMed: 12566415]
12. Larsen MT, Kuhlmann M, Hvam ML, and Howard KA. 2016. Albumin-based drug delivery: harnessing nature to cure disease. Molecular and cellular therapies 4: 3. [PubMed: 26925240]
13. Chen N, Wang W, Fauty S, Fang Y, Hamuro L, Hussain A, and Prueksaritanont T. 2014. The effect of the neonatal Fc receptor on human IgG biodistribution in mice. MAbs 6: 502–508. [PubMed: 24492305]
14. Yip V, Palma E, Tesar DB, Mundo EE, Bumbaca D, Torres EK, Reyes NA, Shen BQ, Fielder PJ, Prabhu S, Khawli LA, and Boswell CA. 2014. Quantitative cumulative biodistribution of antibodies in mice: effect of modulating binding affinity to the neonatal Fc receptor. MAbs 6: 689–696. [PubMed: 24572100]
15. Simecek P, Churchill GA, Yang H, Rowe LB, Herberg L, Serreze DV, and Leiter EH. 2015. Genetic Analysis of Substrain Divergence in Non-Obese Diabetic (NOD) Mice. G3 (Bethesda) 5: 771–775. [PubMed: 25740934]
16. Shultz LD, Lyons BL, Burzenski LM, Gott B, Chen X, Chaleff S, Kotb M, Gillies SD, King M, Mangada J, Greiner DL, and Handgretinger R. 2005. Human lymphoid and myeloid cell development in NOD/LtSz-scid IL2R gamma null mice engrafted with mobilized human hemopoietic stem cells. J Immunol 174: 6477–6489. [PubMed: 15879151]
17. Serr I, Furst RW, Achenbach P, Scherm MG, Gokmen F, Haupt F, Sedlmeier EM, Knopff A, Shultz L, Willis RA, Ziegler AG, and Daniel C. 2016. Type 1 diabetes vaccine candidates promote human Foxp3(+)Treg induction in humanized mice. Nature communications 7: 10991.
18. Rotwein P, Yokoyama S, Didier DK, and Chirgwin JM. 1986. Genetic analysis of the hypervariable region flanking the human insulin gene. American journal of human genetics 39: 291–299. [PubMed: 2876625]
19. Fahey JR, Lyons BL, Olekszak HL, Mourino AJ, Ratiu JJ, Racine JJ, Chapman HD, Serreze DV, Baker DL, and Hendrix NK. 2017. Antibiotic-associated Manipulation of the Gut Microbiota and Phenotypic Restoration in NOD Mice. Comp Med 67: 335–343. [PubMed: 28830580]
20. Julius MH, and Herzenberg LA. 1974. Isolation of antigen-binding cells from unprimed mice: demonstration of antibody-forming cell precursor activity and correlation between precursor and secreted antibody avidities. The Journal of experimental medicine 140: 904–920. [PubMed: 4139227]
21. Serreze DV, Leiter EH, Worthen SM, and Shultz LD. 1988. NOD marrow stem cells adoptively transfer diabetes to resistant (NOD x NON)F1 mice. Diabetes 37: 252–255. [PubMed: 3134263]
22. Michels AW, Landry LG, McDaniel KA, Yu L, Campbell-Thompson M, Kwok WW, Jones KL, Gottlieb PA, Kappler JW, Tang Q, Roep BO, Atkinson MA, Mathews CE, and Nakayama M. 2017. Islet-Derived CD4 T Cells Targeting Proinsulin in Human Autoimmune Diabetes. Diabetes 66: 722–734. [PubMed: 27920090]
23. Pathiraja V, Kuehlich JP, Campbell PD, Krishnamurthy B, Loudovaris T, Coates PT, Brodnicki TC, O'Connell PJ, Kedzierska K, Rodda C, Bergman P, Hill E, Purcell AW, Dudek NL, Thomas HE, Kay TW, and Mannering SI. 2015. Proinsulin-specific, HLA-DQ8, and HLA-DQ8-transdimer-restricted CD4+ T cells infiltrate islets in type 1 diabetes. Diabetes 64: 172–182. [PubMed: 25157096]
24. Zhumabekov T, Corbella P, Tolaini M, and Kioussis D. 1995. Improved version of a human CD2 minigene based vector for T cell-specific expression in transgenic mice. J Immunol Methods 185: 133–140. [PubMed: 7665895]
25. Sawada S, Scarborough JD, Killeen N, and Littman DR. 1994. A lineage-specific transcriptional silencer regulates CD4 gene expression during T lymphocyte development. Cell 77: 917–929. [PubMed: 8004678]
26. Johnson EA, Silveira P, Chapman HD, Leiter EH, and Serreze DV. 2001. Inhibition of autoimmune diabetes in nonobese diabetic mice by transgenic restoration of H2-E MHC class II expression:

additive, but unequal, involvement of multiple APC subtypes. J Immunol 167: 2404–2410. [PubMed: 11490031]

27. Ratiu JJ, Racine JJ, Hasham MG, Wang Q, Branca JA, Chapman HD, Zhu J, Donghia N, Philip V, Schott WH, Wasserfall C, Atkinson MA, Mills KD, Leeth CM, and Serreze DV. 2017. Genetic and Small Molecule Disruption of the AID/RAD51 Axis Similarly Protects Nonobese Diabetic Mice from Type 1 Diabetes through Expansion of Regulatory B Lymphocytes. J Immunol 198: 4255–4267. [PubMed: 28461573]
28. Shimizu J, Yamazaki S, Takahashi T, Ishida Y, and Sakaguchi S. 2002. Stimulation of CD25(+)CD4(+) regulatory T cells through GITR breaks immunological self-tolerance. Nature immunology 3: 135–142. [PubMed: 11812990]
29. Bennett ST, and Todd JA. 1996. Human type 1 diabetes and the insulin gene: principles of mapping polygenes. Annu Rev Genet 30: 343–370. [PubMed: 8982458]
30. Jansen A, Rosmalen JG, Homo-Delarche F, Dardenne M, and Drexhage HA. 1996. Effect of prophylactic insulin treatment on the number of ER-MP23+ macrophages in the pancreas of NOD mice. Is the prevention of diabetes based on beta-cell rest? Journal of autoimmunity 9: 341–348. [PubMed: 8816969]
31. Rosmalen JG, Homo-Delarche F, Durant S, Kap M, Leenen PJ, and Drexhage HA. 2000. Islet abnormalities associated with an early influx of dendritic cells and macrophages in NOD and NODscid mice. Laboratory investigation; a journal of technical methods and pathology 80: 769–777. [PubMed: 10830787]
32. Gaskins HR, Prochazka M, Hamaguchi K, Serreze DV, and Leiter EH. 1992. Beta cell expression of endogenous xenotropic retrovirus distinguishes diabetes-susceptible NOD/Lt from resistant NON/Lt mice. The Journal of clinical investigation 90: 2220–2227. [PubMed: 1361492]
33. Mingueneau M, Jiang W, Feuerer M, Mathis D, and Benoist C. 2012. Thymic negative selection is functional in NOD mice. The Journal of experimental medicine 209: 623–637. [PubMed: 22329992]
34. Katz JD, Wang B, Haskins K, Benoist C, and Mathis D. 1993. Following a diabetogenic T cell from genesis through pathogenesis. Cell 74: 1089–1100. [PubMed: 8402882]
35. Jasinski JM, Yu L, Nakayama M, Li MM, Lipes MA, Eisenbarth GS, and Liu E. 2006. Transgenic insulin (B:9–23) T-cell receptor mice develop autoimmune diabetes dependent upon RAG genotype, H-2g7 homozygosity, and insulin 2 gene knockout. Diabetes 55: 1978–1984. [PubMed: 16804066]
36. Anderson AM, Landry LG, Alkanani AA, Pyle L, Powers AC, Atkinson MA, Mathews CE, Roep BO, Michels AW, and Nakayama M. 2021. Human islet T cells are highly reactive to preproinsulin in type 1 diabetes. Proceedings of the National Academy of Sciences of the United States of America 118.
37. Gascoigne NR, and Alam SM. 1999. Allelic exclusion of the T cell receptor alpha-chain: developmental regulation of a post-translational event. Seminars in immunology 11: 337–347. [PubMed: 10497088]
38. Jing Y, Kong Y, McGinty J, Blahnik-Fagan G, Lee T, Orozco-Figueroa S, Bettini ML, James EA, and Bettini M. 2022. T-Cell Receptor/HLA Humanized Mice Reveal Reduced Tolerance and Increased Immunogenicity of Posttranslationally Modified GAD65 Epitope. Diabetes 71: 1012–1022. [PubMed: 35179565]
39. Elliott JF, Liu J, Yuan ZN, Bautista-Lopez N, Wallbank SL, Suzuki K, Rayner D, Nation P, Robertson MA, Liu G, and Kavanagh KM. 2003. Autoimmune cardiomyopathy and heart block develop spontaneously in HLA-DQ8 transgenic IAbeta knockout NOD mice. Proceedings of the National Academy of Sciences of the United States of America 100: 13447–13452. [PubMed: 14570980]
40. Taneja V, and David CS. 2009. Spontaneous autoimmune myocarditis and cardiomyopathy in HLA-DQ8.NODAbo transgenic mice. Journal of autoimmunity 33: 260–269. [PubMed: 19811893]
41. Taylor JA, Havari E, McInerney MF, Bronson R, Wucherpfennig KW, and Lipes MA. 2004. A spontaneous model for autoimmune myocarditis using the human MHC molecule HLA-DQ8. J Immunol 172: 2651–2658. [PubMed: 14764740]

42. Pascolo S, Bervas N, Ure JM, Smith AG, Lemonnier FA, and Perarnau B. 1997. HLA-A2.1-restricted education and cytolytic activity of CD8(+) T lymphocytes from beta2 microglobulin (beta2m) HLA-A2.1 monochain transgenic H-2Db beta2m double knockout mice. The Journal of experimental medicine 185: 2043–2051. [PubMed: 9182675]

Key Points

Creation of ten new HLA-humanized NOD strains with or without chimeric human TCRs.

NOD T-cells with human murine or human insulin-reactive TCRs infiltrate islets.

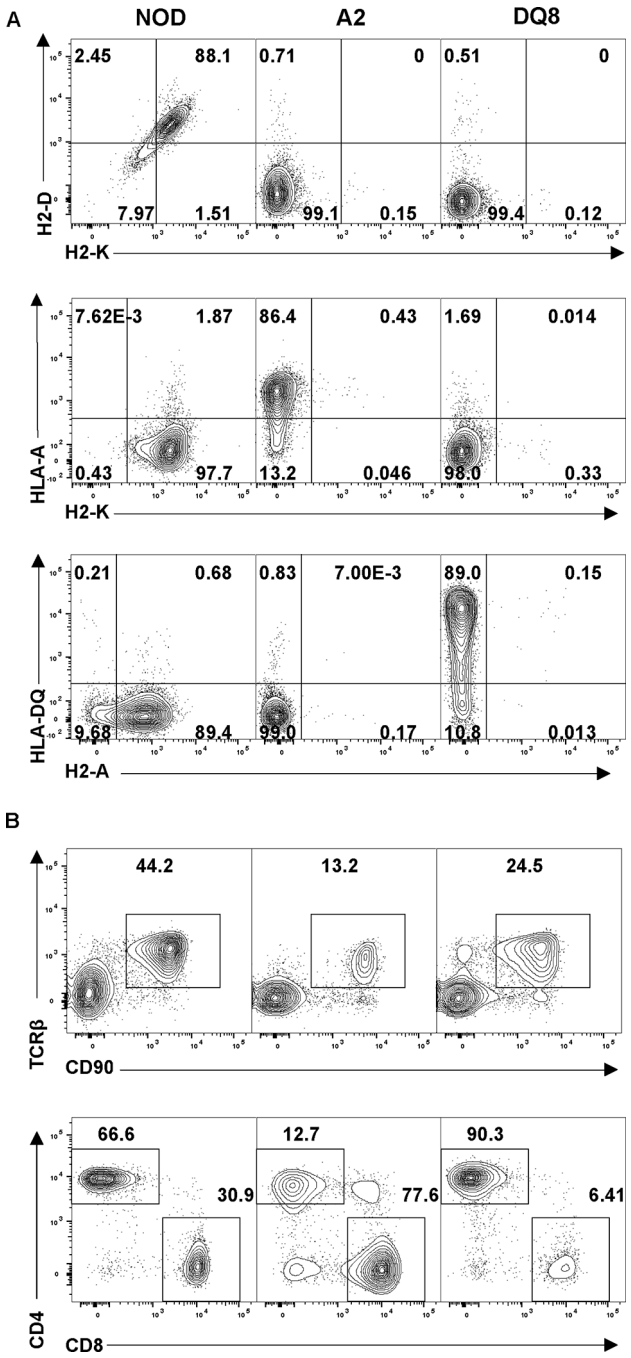

Figure 1 –. Creation of NOD-*cMHCI/II*$^{-/-}$-A2 and NOD-*cMHCI/II*$^{-/-}$.DQ8 Mice

(A) Splenocytes from 8–10-week-old male NOD, NOD-*cMHCI/II*$^{-/-}$-A2, and NOD-*cMHCI/II*$^{-/-}$.DQ8 mice were examined for murine MHC I expression **(H2-D/H2-K, Top)**, human MHC I expression **(HLA-A, Middle)**, murine H2-A or human HLA-DQ MHC II expression **(Bottom)** on gated live B220^{+} B-cells. Representative flow cytometry patterns from one of 5 individuals examined per strain. **(B)** Splenocytes from the same mice in A, showing CD90^{+} TCRβ^{+} amongst live cells **(Top)** and CD4^{+} or CD8^{+} amongst gated

$CD90^+$ $TCR\beta^+$ **(Bottom)**. Representative flow cytometry patterns from one of 5 individuals examined per strain.

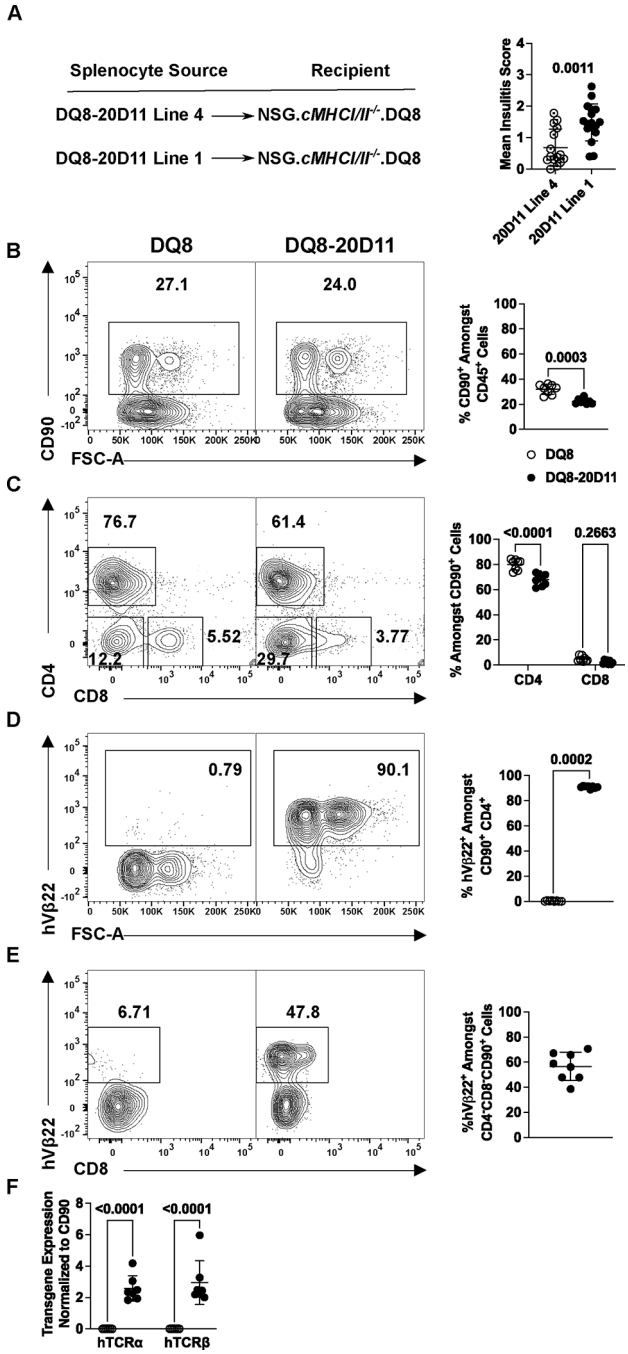

Figure 2 - Creation of NOD-*cMHCI/II*$^{-/-}$.DQ8–20D11 Mice

(A) Male and female NSG-*cMHCI/II*$^{-/-}$.DQ8 mice were injected with 10×10^6 whole splenocytes from sex-matched NOD-*cMHCI/II*$^{-/-}$.DQ8–20D11 Line 1 or Line 4 donors **(Left – schematic)**. Mean insulitis score thirty weeks after transfer showing Mean±SD of 15–17 mice per group **(Right)**. **(B)** Representative splenic flow cytometry patterns **(Left)** and quantification **(Right)** of CD90$^+$ cells amongst live CD45$^+$ cells. **(C)** Representative splenic flow cytometry patterns **(Left)** and quantification **(Right)** of %CD4 and %CD8 amongst gated CD90$^+$ cells. **(D)** Representative splenic flow cytometry patterns **(Left)** and

quantification **(Right)** of %hVβ22 amongst gated $CD90^+$ $CD4^+$ cells. **(E)** Representative splenic flow cytometry patterns **(Left)** and quantification **(Right)** of %hVβ22 amongst gated $CD90^+$ $CD4^-$ $CD8^-$ cells. Data in A is from N=4 separate cellular preparations per line. All data **(B-E)** combined from two experiments of n=8 10-week-old females per group. **(F)** $CD4^+$ T-cells were negatively enriched in two separate experiments. Data showing human transgenic TCRα and TCRβ normalized to CD90 expression in each DQ8 or DQ8–20D11 sample. All quantification dot plots showing Mean±SD, N=6–7 mice per group.

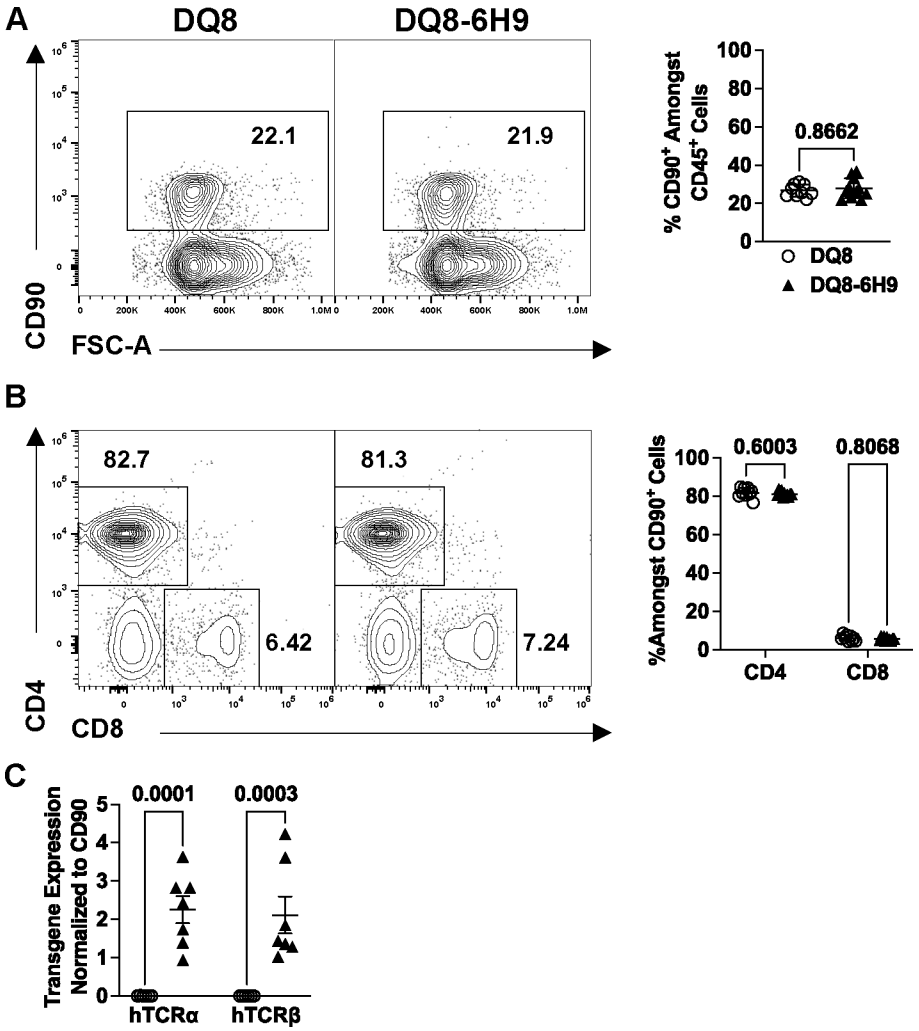

Figure 3 - Creation of NOD-*cMHCI/II*$^{-/-}$.DQ8–6H9 Mice

(A) Representative splenic flow cytometry pattern **(Left)** and quantification **(Right)** of %CD90^{+} amongst live cells. **(B)** Representative splenic flow cytometry pattern **(Left)** and quantification **(Right)** of %CD4^{+} and %CD8^{+} amongst live CD90^{+} cells. For both panels, 8–10-week-old male and female mice were examined. A total of 9–11 mice were examined for both strains across three experiments. Quantification plots show Mean±SD. **(C)** Expression of human transgenic TCRα and TCRβ mRNA on negatively enriched CD4^{+} T-cells (N=6–7 mice per group, enriched in two separate experiments). Data is normalized to CD90 expression within the sample.

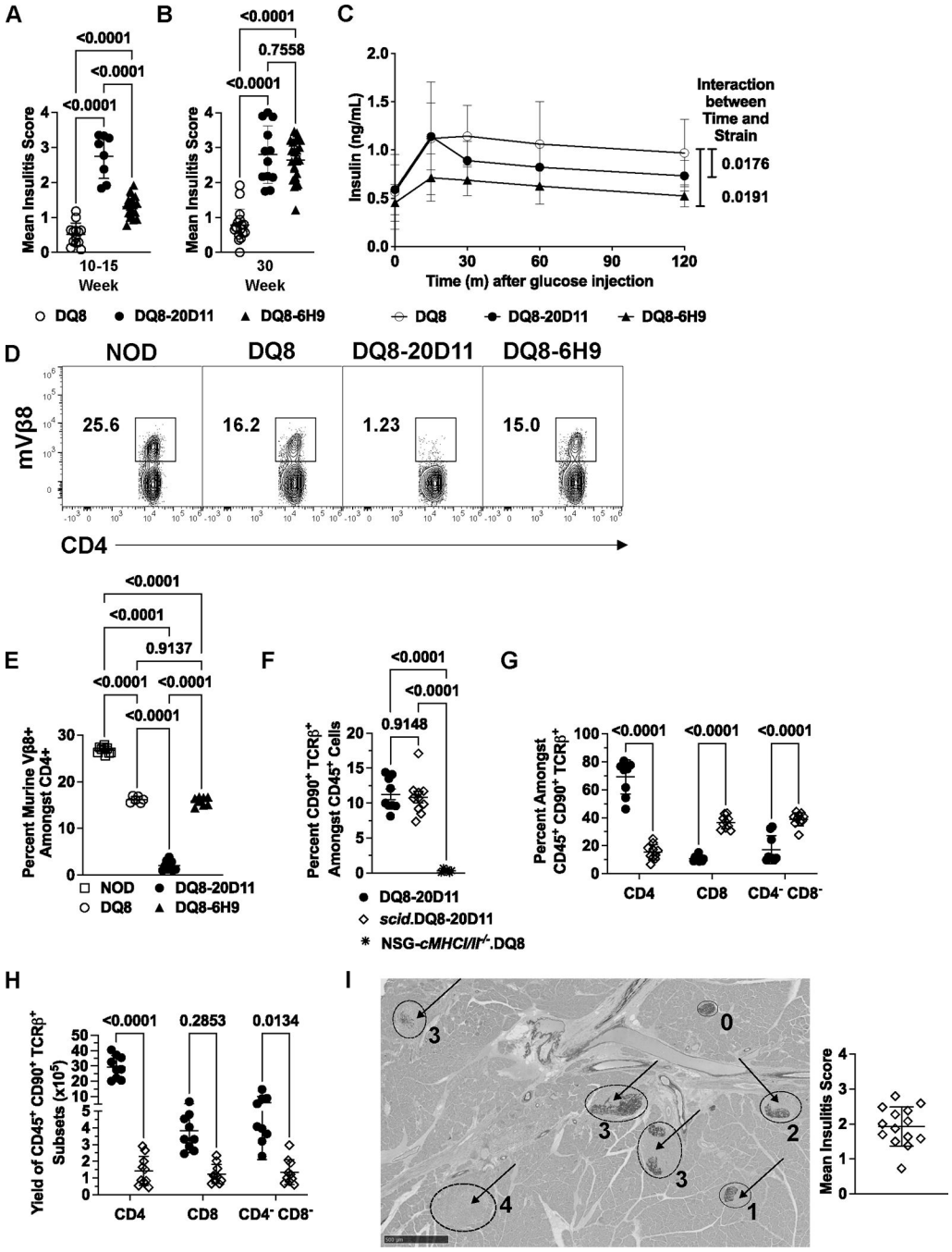

Figure 4 –. 20D11 and 6H9 Transgenic T-cells Cause Insulitis with Differing Kinetics And T-cell Development Outcomes

Mean insulitis scores (Mean±SD) at 10–15 weeks (8–16 mice per group) **(A)** or 30 weeks of age (N=12–24) **(B)** in NOD-*cMHCI/II*$^{-/-}$.DQ8, NOD-*cMHCI/II*$^{-/-}$.DQ8–20D11 and NOD-*cMHCI/II*$^{-/-}$.DQ8–6H9 female mice. **(C)** Quantification of plasma insulin at various timepoints after exogenous glucose administration. Displayed p-value derived from two-way ANOVA's showing Time x Strain interaction comparing indicated hTCR strains to DQ8 parental mice (N=8 mice per strain; 12.9–15 weeks of age; two experiments). **(D-E)**

Representative staining **(D)** and quantification **(E)** of percent Vβ8$^+$ amongst live CD4$^+$ cells comparing NOD, DQ8, DQ8–20D11 and DQ8–6H9 mice. **(F)** Quantification of percent CD90$^+$ TCRβ$^+$ amongst live CD45$^+$ splenocytes. **(G)** Quantification of T-cell subsets amongst CD45$^+$ CD90$^+$ TCRβ$^+$ splenocytes. **(H)** Yield of T-cell subsets. All data shows Mean±SD. For **D-H** all data is combined from two experiments. **(I)** Representative H&E and aldehyde fuchsin stained islet histology image **(Left)** and quantification of mean insulitis scores (Mean±SD) **(Right)** at 20 weeks for *scid*.DQ8–20D11 mice. Dashed circles show rough shape of residual islets; arrows indicate areas of immune cell infiltrate; the darker-stained sections within islets are aldehyde fuchsin staining of residual insulin producing β-cells. Numbers next to circled islets indicate score assigned by blinded observer for that individual islet. Scale bar shows 500μm.

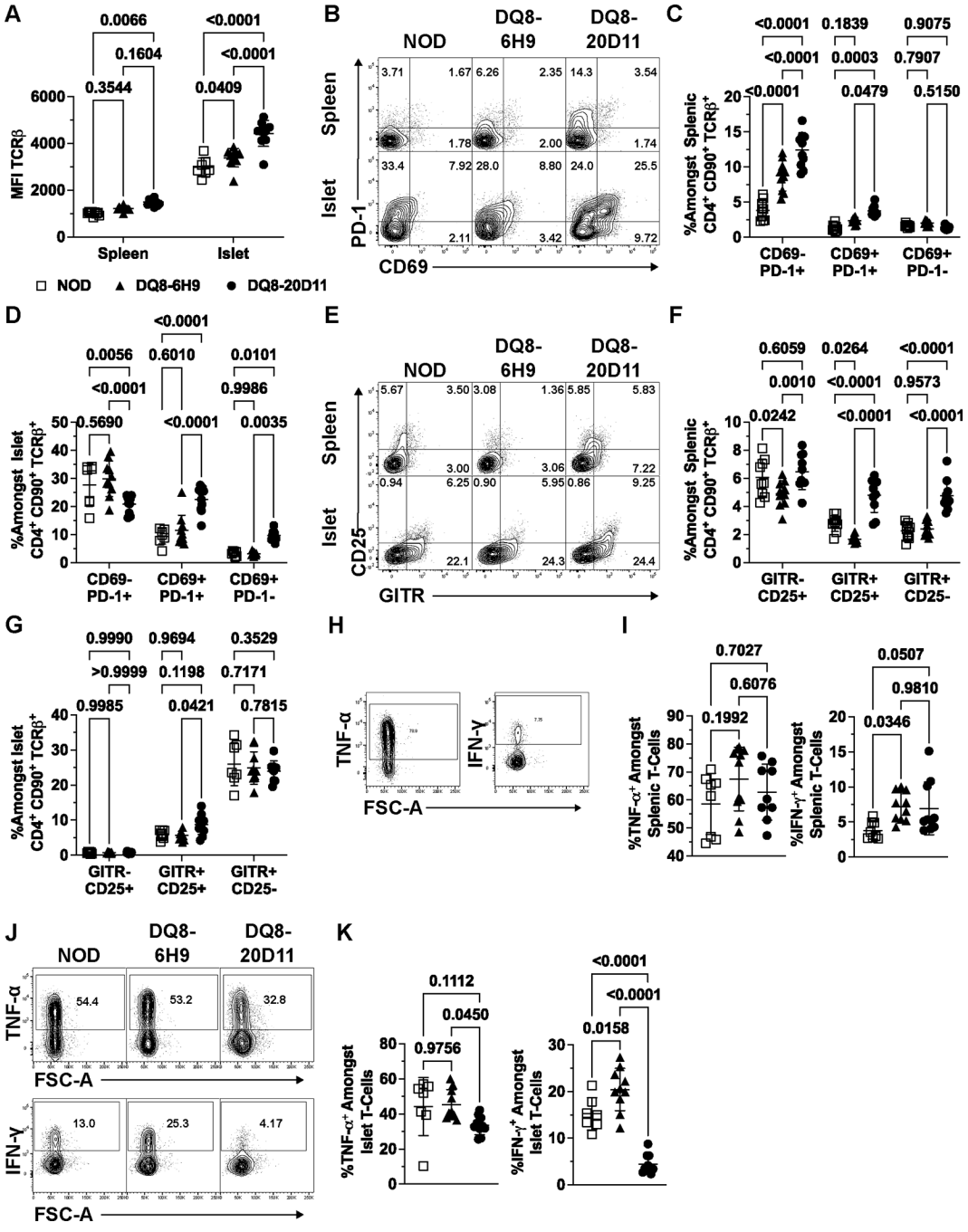

Figure 5 –. hTCR T-cells Display Varying Levels of Activation and Tolerance Within Islets

(A) MFI of TCRβ on splenic and islet T-cells. **(B-D)** Representative staining **(B)** and quantification **(C, D)** of CD69 versus PD-1 on gated CD4$^+$ CD90$^+$ TCRβ$^+$ cells from spleen **(C)** and islets **(D)**. **(E-G)** Representative staining **(E)** and quantification **(F, G)** of GITR versus CD25 on gated CD4$^+$ CD90$^+$ TCRβ$^+$ cells from spleen **(F)** and islets **(G)**. **(H-K)** Representative staining **(H, J)** and quantification **(I, K)** of TNF-α and IFN-γ on gated CD4$^+$ CD90$^+$ splenic **(H, I)** and islet derived T-cells **(J, K)**. **(H)** displays a single DQ8–6H9 mouse

for representative gating of splenocytes, while **(J)** displays a representative of islet T-cells from each strain. All data shows Mean±SD combined from two experiments.

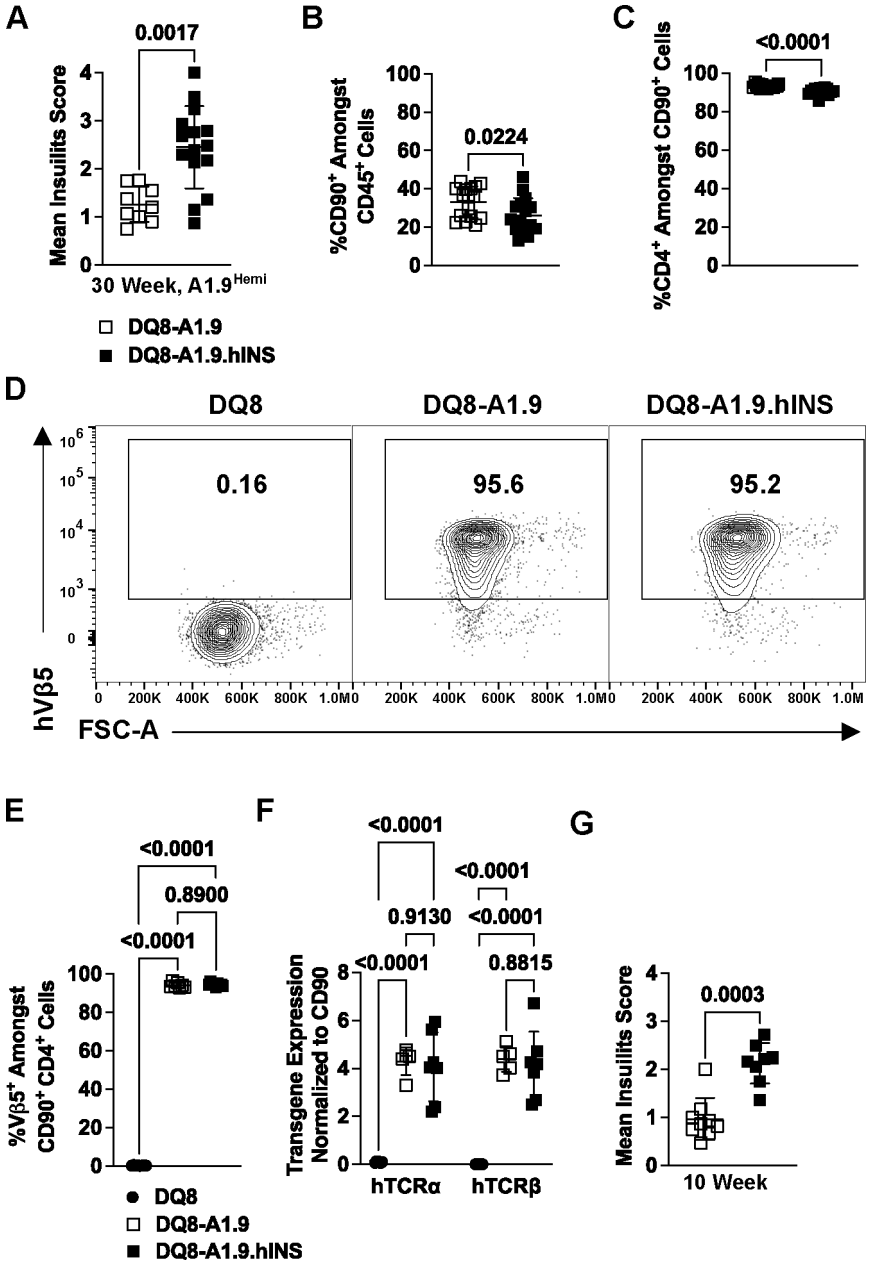

Figure 6 –. A1.9 Transgenic T-cells Cause Insulitis in Mice with Human Insulin Expression

(A) Mean insulitis scores at 30 weeks of age in NOD-*cMHCI/II*$^{-/-}$.DQ8-A1.9$^{Tg/0}$ female mice with and without human insulin expression (N=9–15). **(B-C)** Quantification of %CD90^{+} amongst live splenocytes **(B),** %CD4^{+} amongst CD90^{+} splenocytes **(C)**. N=16–17 8–10-week-old mice (male and female) per strain combined from two experiments. **(D-E)** Representative flow cytometry plot **(D)** and quantification **(E)** of %hVβ5 amongst gated CD90^{+} CD4+ splenocytes. N=7–9 8–10-week-old male mice per strain (one experiment). **(F)** CD4^{+} T-cells were negatively enriched across two experiments (N=5–7 mice per group). Data showing human transgenic TCRα and TCRβ mRNA expression normalized to CD90 expression in each DQ8, DQ8-A1.9, or A1.9-hINS sample. **(G)** Mean insulitis scores for

female NOD-*cMHCI/II*$^{-/-}$.DQ8-A1.9$^{Tg/Tg}$ mice with or without hINS at 10 weeks of age (N=8–9). All data shows Mean±SD.

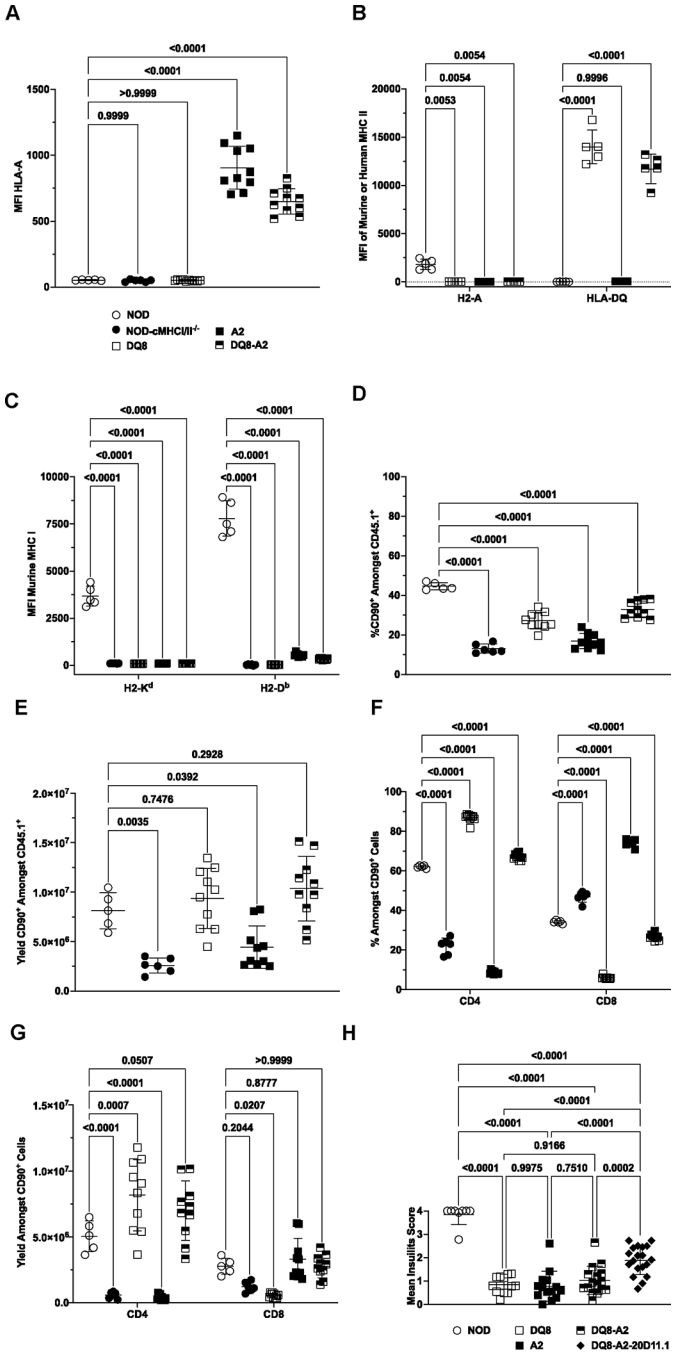

Figure 7 - Creation of NOD-*cMHCI/II*$^{-/-}$.DQ8-A2 mice

Eight-ten-week-old male and female were examined by flow cytometry of splenic cells. Median fluorescence intensity (MFI) of HLA-A **(A)**, H2-A and HLA-DQ **(B)** and H2-K and H2-D **(C)** on splenic B220^{+} cells. Percent **(D)** and yield **(E)** of CD90^{+} cells. Percent **(F)** and yield **(G)** of CD4^{+} and CD8^{+} cells. **(H)** Mean insulitis scores of female mice at 30 weeks of age. All data show Mean±SD. Quantification in panels A-G is combined from two

experiments with the exception of panel B, which are data from one representative (of two) experiments. N=5–10 mice per strain.

Table I:

Human TCR sequence information

Clone	TRAV	TRAJ	TRA CDR3	TRBV	TRBJ	TRBD	TRB CDR3	Target
20D11	12-3*01	4*01	CAILSGGYNKLIF	2*01	2-5*01		CASSAETQYF	Insulin $B_{9–23}$
6H9	26-1*02	40*01	CIVRVDSGTYKYIF	7-2*02	2-1*01		CASSLTAGLASTYNEQFF	Insulin $B_{9–23}$
A1.9	20*02	7*01	CAVQAGGNNRLAF	5–1*01	1–2*01	1*01	CASSLERDGYTF	Human C-peptide$_{42–50}$

Table II:

qPCR Primers and probes for Genotyping hTCR transgenes

Tcra Primers and Probes				
Target	**Primer Name**	**5' label**	**5' – Sequence – 3'**	**3' label**
hCD2 Sequence Common to: 20D11, 6H9, A1.9	Tg F (hCD2)		TGA CTC TCA GTA ACT CTT TTG CT	
Tcra Sequence Common to: 20D11, 6H9	Tg R (20D11Tcra)		ATA ATG TAG GAG CAT ATG TTT TCA TGG	
Probe for 20D11, 6H9	Tg Probe	[6-FAM]	AGG TGC AGT CTC CAA AGG CCA	[BHQ1a-Q]
Tcra A1.9	Tg R (TRAV)		GCA CAC TCC AAC ATT TTC TCC	
Probe for A1.9	Tg Probe	[6-FAM]	TGC AGT CTC CAA AGA ATT GCC GC	[BHQ1a-Q]
Tcrb Primers and Probes				
Target	**Primer Name**	**5' label**	**5' – Sequence – 3'**	**3' label**
mCd4 Sequence Common to: 20D11, 6H9, A1.9	Tg F (mCd4)		TTG TAG GCT CAG ATT CCC AAC	
Tcrb Sequence Common to: 20D11, 6H9	Tg R (Tcrb)		ACA AGA CAT AGG GAA ACA TAG AGG	
Probe for 20D11, 6H9	Tg Probe	[6-FAM]	CCA CCA TGA GCT GCA GGC TTC T	[BHQ1a-Q]
Tcrb A1.9	Tg R (TCRbeta)		AGC ACC CAA CAG AGC AG	
Probe for A1.9	Tg Probe	[6-FAM]	TCA AGG AGT CGA GCC GCC AC	[BHQ1a-Q]
Controls	Apob control F		CAC GTG GGC TCC AGC ATT	
	Apob control R		TCA CCA GTC ATT TCT GCC TTT G	
	Apob controlPR	[Cy5]	CCA ATG GTC GGG CAC TGC TCA A	[BHQ2a-Q]

Table III:

New Humanized NOD Mouse Models

Short Name	*H2-K1* Allele	*H2-Ab1* Allele	*H2-D1* Allele	*Prkdc* Allele	*Il2rg* Allele	HLA-DQ8	HLA-A2*0201	Human TCR Allele	Human Insulin
NSG-*Ab0*-DQ8-INS*VNTR	*b*	*b-tm1Doi*	*b*	*scid*	*tm1Wjl*	Yes	No	None	Yes
DQ8	*d-em1Dvs*	*g7-em1Dvs*	*b-em5Dvs*	*wt*	*wt*	Yes	No	None	No
DQ8-20D11	*d-em1Dvs*	*g7-em1Dvs*	*b-em5Dvs*	*wt*	*wt*	Yes	No	Tg(CD2-Tcra20D11,Cd4-Tcrb20D11)1Dvs	No
DQ8-6H9	*d-em1Dvs*	*g7-em1Dvs*	*b-em5Dvs*	*wt*	*wt*	Yes	No	Tg(CD2-Tcra6H9,Cd4-Tcrb6H9)2Dvs	No
DQ8-A1.9	*d-em1Dvs*	*g7-em1Dvs*	*b-em5Dvs*	*wt*	*wt*	Yes	No	Tg(CD2-TcraA1.9,Cd4-TcrbA1.9)1Dvs	No
DQ8-A1.9.hINS	*d-em1Dvs*	*g7-em1Dvs*	*b-em5Dvs*	*wt*	*wt*	Yes	No	Tg(CD2-TcraA1.9,Cd4-TcrbA1.9)1Dvs	Yes
NSG-*cMHCI/II*$^{-/-}$.DQ8	*d-em1Dvs*	*g7-em1Dvs*	*b-em5Dvs*	*scid*	*tm1Wjl*	Yes	No	None	No
***scid*.DQ8-20D11**	*d-em1Dvs*	*g7-em1Dvs*	*b-em5Dvs*	*scid*	*wt*	Yes	No	Tg(CD2-Tcra20D11,Cd4-Tcrb20D11)1Dvs	No
A2	*d-em1Dvs*	*g7-em1Dvs*	*b-em5Dvs*	*wt*	*wt*	No	Yes	None	No
DQ8-A2	*d-em1Dvs*	*g7-em1Dvs*	*b-em5Dvs*	*wt*	*wt*	Yes	Yes	None	No
DQ8-A2-20D11	*d-em1Dvs*	*g7-em1Dvs*	*b-em5Dvs*	*wt*	*wt*	Yes	Yes	Tg(CD2-Tcra20D11,Cd4-Tcrb20D11)1Dvs	No

Formal strain designations are presented in the Methods Section

Note: NSG-*Ab0*-DQ8-INS*VNTR is a publicly available, previously unpublished, mouse model available from The Jackson Laboratory (Strain #: 026936)